NASA Technical Memorandum 81363

(NASA-TM-81363) PRELIMINARY ANALYSIS OF STS-1 ENTRY FLIGHT DATA (NASA) 73 p
HC A04/MF A01 CSCL 22B

N81-29153

Unclas
G3/18 27073

PRELIMINARY ANALYSIS OF STS-1 ENTRY FLIGHT DATA

August 1981

NASA

NASA Technical Memorandum 81363

PRELIMINARY ANALYSIS OF STS-1 ENTRY FLIGHT DATA

Dryden Flight Research Center
Edwards, California

1981

NOMENCLATURE

Acronyms

ACIP	aerodynamic coefficient identification package
AFFTC	Air Force Flight Test Center
ALT	approach and landing tests
ASKA	automatic system for kinematic analysis
CSS	control stick steering
DFI	development flight instrumentation
DFRC	Dryden Flight Research Center
FS	fuselage station
GNC	guidance, navigation, and control
GPC	general purpose computer
HUD	heads-up display
JSC	Johnson Space Center
MMLE	modified maximum likelihood estimation
NAV	navigation
OI	operational instrumentation
OV	orbiter vehicle
PIO	pilot-induced oscillation
PKQ	suppression factor
PST	Pacific standard time
PTI	programmed test input
RCS	reaction control system
RHC	rotational hand controller
RSI	reusable surface insulation
RI	Rockwell International
SPAR	structural performance and resizing

STS	space transportation system
TPS	thermal protection system
VEAS	velocity equivalent airspeed, knots
WS	wing station

Symbols

a_{ℓ}	longitudinal acceleration, g
a_n	normal acceleration, g
a_x	longitudinal acceleration, g
a_y	lateral acceleration, g
BF	body flap, deg
b	span, ft
C_{ℓ}	rolling moment/$\bar{q}Sb$
$C_{\ell_{\delta_a}}$	$= \frac{\partial C_{\ell}}{\partial \delta_a}$
$C_{\ell_{\beta}}$	$= \frac{\partial C_{\ell}}{\partial \beta}$
C_m	pitching moment/$\bar{q}S\bar{c}$
$C_{m_{\alpha}}$	$= \frac{\partial C_m}{\partial \alpha}$
$C_{m_{\delta_e}}$	$= \frac{\partial C_m}{\partial \delta_e}$
$C_{m_{BF}}$	$= \frac{\partial C_m}{\partial BF}$
C_n	yawing moment/$\bar{q}Sb$

C_{n_β} $= \frac{\partial C_n}{\partial \beta}$

$C_{n_{\delta_a}}$ $= \frac{\partial C_n}{\partial \delta_a}$

C_y yawing moment/$\bar{q}S$

$C_{y_{\delta_a}}$ $= \frac{\partial C_y}{\partial \delta_a}$

C_{y_β} $= \frac{\partial C_y}{\partial \beta}$

$\bar{c}$ mean aerodynamic chord, ft

D drag, lb

h altitude

L/D lift to drag ratio

L_r rolling moment due to yaw rate

L_{YJ} rolling moment due to yaw jet

L_{δ_r} rolling moment due to rudder

M Mach number

N_{YJ} yawing moment due to yaw jet

q pitch velocity, deg/sec

$\bar{q}$ dynamic pressure, psf

S wing area, ft^2

t_o plot start time (Greenwich mean time)

V velocity

x body axis longitudinal coordinate

Y_{YJ} yawing force due to yaw jets

y	body axis spanwise coordinate
z	body axis vertical coordinate
α	angle of attack, deg
β	angle of sideslip, deg
δ_a	aileron deflection, deg
δ_e	elevator position, deg
$\dot{\delta}_e$	$= \frac{\partial \delta_e}{\partial t}$
δ_r	rudder position
θ	pitch angle
ϕ	roll angle

INTRODUCTION

Dryden has completed a first look at the data obtained during entry of the STS-1 flight. Our efforts so far have been concentrated in the areas in which we conducted our preflight analysis and predictions with the intent to independently assess the flight results of STS-1.

In this report, Section I contains heating results for the few parameters that were available in real time. The recorded channels of data are not yet available in usable form.

Section II presents preliminary results of the performance, trim, and control usage. Variations in measured versus predicted L/D and trim are discussed, as well as plots showing time histories of control surface and jet activity.

Section III presents a comparison of the derivatives extracted from flight with those predicted.

Section IV presents a discussion of several flight anomalies along with a brief analysis of the landing.

Section V presents the concluding remarks and a summary of recommendations.

Finally, Section VI briefly describes the sources of the data used in this report.

SECTION I - ENTRY HEATING ANALYSIS

Background

The DFRC Structures Branch is assisting JSC in OV-102 strain gage airload measurement. As a part of this task, corrections for thermal stress effects must be established. Both empirical and analytical approaches are being pursued.

For the analytical approach, two dimensional thermal stress analysis models for each strain gaged cross section were generated and checked against the contractor's ASKA model results. Since there are insufficient flight measurements to establish the structural temperature distribution at these cross sections, SPAR full cross section thermal models were generated to provide analytical estimates. Initially, models of fuselage cross section FS 877 and wing cross section WS 240, located as shown in figure 1, were assembled. The aluminum substructure was modeled in considerable detail, as shown in figure 2. The TPS was modeled in 10 layers on the lower surface and three to four layers on the upper surface. Only 80% of the TPS thickness was used to account for gap heating, based on ground test results. For preflight estimates, heating was generated using traditional methods, assuming pure turbulent and pure laminar attached boundary layer conditions, to produce upper and lower bounds on the flight measured data. The plan for postflight analysis is to establish the correct heating from flight data, compute structural temperatures from the heat transfer models and compare with available structural temperature measurements for validation of the analysis procedure. The heat transfer models will be adjusted to produce a good correlation with available flight test measurements. The heat transfer model results will then be entered into the thermal stress analysis models to compute thermal corrections for the flight measured strains.

Comparison of Results

To gain early insight, DFRC developed the capability for acquisition and display of some of the DFI telemetered data. Of the parameters selected for real time display, seven were structural temperature measurements, four at FS 877 and three at WS 240. Prior to flight, RI predictions for these measurements were obtained for comparison, along with DFRC predicted values.

The selected measurements for the fuselage station are shown in figure 3. Figures 4 to 7 are time history plots of flight measured temperatures compared to DFRC and RI predictions. The time is measured from entry, which is defined to occur at a 400,000-foot altitude (PST 9:48:55). Telemetered data could not be acquired until 10:08:32 or 1177 seconds into the entry profile (labeled "end of blackout" in the figures). Only the sidewall temperature exceeded RI predictions. The bottom temperature followed the laminar prediction quite closely, while the lower glove measured value was far below laminar, which should be the theoretical minimum for attached flow.

The locations of structural temperature measurements for WS 240 are shown in figure 8. Again the measured values (figs. 9 to 11) were considerably less than design predictions. The spar and rib cap values followed the laminar (80% TPS thickness) curves quite closely, but the skin temperature was below laminar

Because of these anomalies, temperatures for the balance of the locations shown in figure 8 were tabulated from the DFI telemetered data after flight. Figures 12 to 14 are time histories of the remaining lower skin temperatures. Again, the measured values were less than laminar (80% TPS thickness). Figure 15 shows the measured results for the lower rear spar cap (1365) which are higher than laminar (80% TPS thickness). The predicted values for the rear spar may be low due to the assumption of total insulation on the aft side of the spar web.

Figures 16 to 19 are time histories of upper wing skin temperatures. Except for the first bay, the measured values are far below the laminar attached flow predictions. The same is true of the upper spar and rib cap measurements (figs. 20 to 22). These upper surface temperatures tend to verify the contention that flow separation is present over a large part of the wing upper surface at high angles of attack during reentry.

The chordwise distribution of WS 240 structural temperatures is shown in figure 23 for time 10:15:35 (profile time 1600) The scalloped shape reflects the drop in temperature at the spar caps. For the lower surface, the chordwise distribution follows the laminar predicted values quite well, except at the rear spar. The upper surface plot shows the effect of separated flow on the aft three bays.

The differences between measured and predicted could be caused by:

a) assumptions in the aero heating analysis (turbulent vs. laminar, attached vs separated, nominal trajectory).

b) assumptions in heat transfer modeling (TPS effective thickness, conductivity, emissivity, internal convection, internal insulation).

The DFI onboard tape malfunctioned for descent, so no DFI data prior to telemetry lock-on will be available for STS-1. A copy of the OI onboard tape was obtained and processed at DFRC, giving a check on the entry profile and giving additional data for one lower wing skin temperature (sensor number V09T9147), as shown in figure 9 Figure 24 compares measured and nominal profile time histories for speed, altitude, and angle of attack. Both NAV and GNC angle of attack measurements are shown, and there is some difference between the measured values. Postflight heating analyses, using the measured profile parameters, did not give significantly different heating than the nominal trajectory.

In a further attempt to establish a lower bound, the WS 240 thermal model was rerun using 100% TPS thickness, and upper surface heating on the last three bays was reduced to account for flow separation. These results are shown on the wing plots (figs. 9 to 22) and the chordwise plot (fig. 23). For the lower surface, the predictions were far too low, but agreement on the upper surface was close.

Current Status

It appears that to obtain sufficiently accurate definition of the internal structural temperatures for generation of strain gage load measurement thermal corrections, a better understanding of external heating, TPS effectiveness, internal emissivity, and convection are required. Unfortunately, the critical surface temperature and pressure data during the first 1000 seconds of reentry were not recovered on STS-1.

For the present we will use the following:

a) for the lower wing surface use the 80% TPS thickness, laminar flow predictions modified by flight data comparison factors.

b) for the upper wing surface use the 100% TPS thickness, separated flow predictions modified by flight data comparison factors.

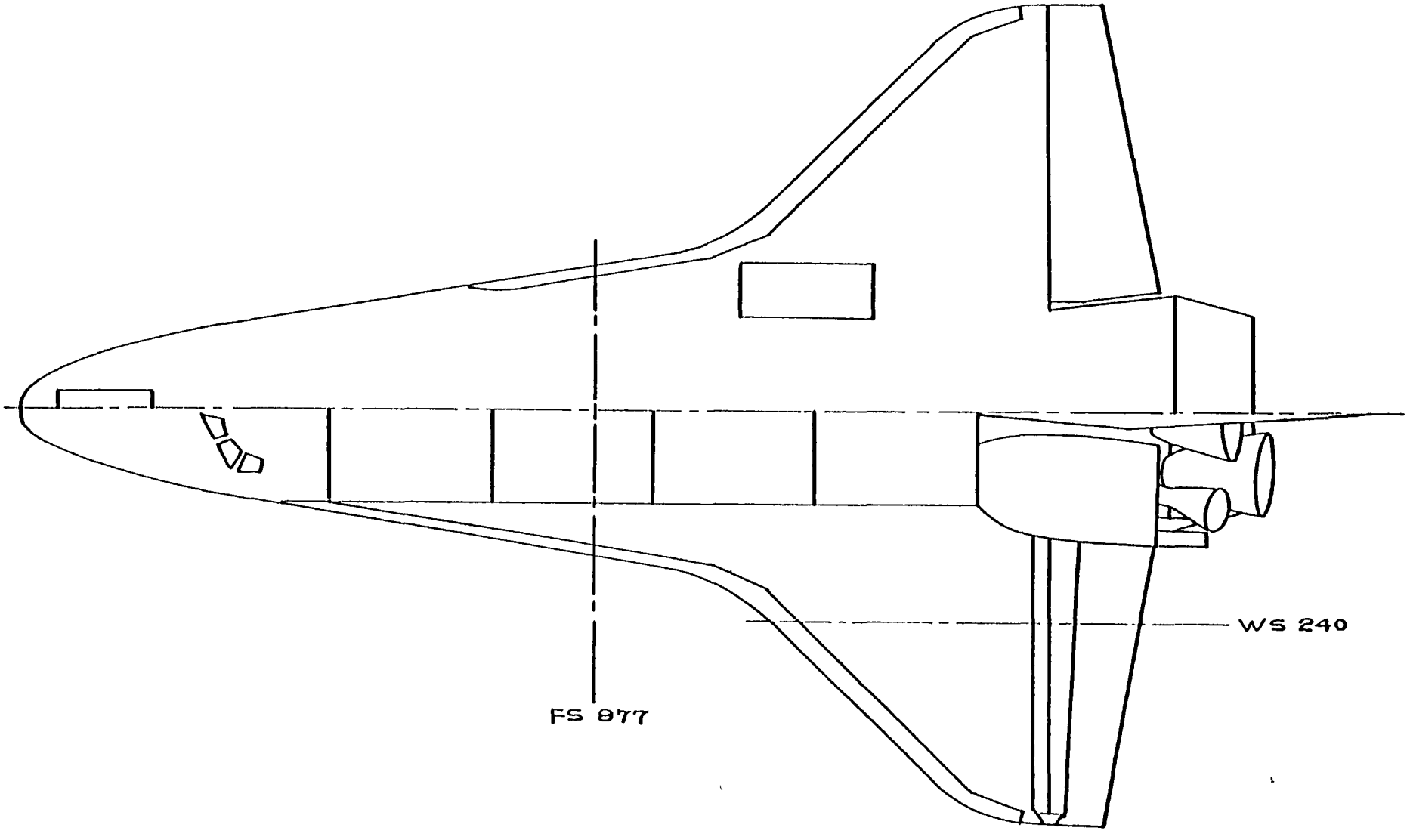

LOCATIONS OF WING STATION WS 240 AND FUSELAGE STATION FS 877.

Figure 1. Thermal Analysis Cross Sections

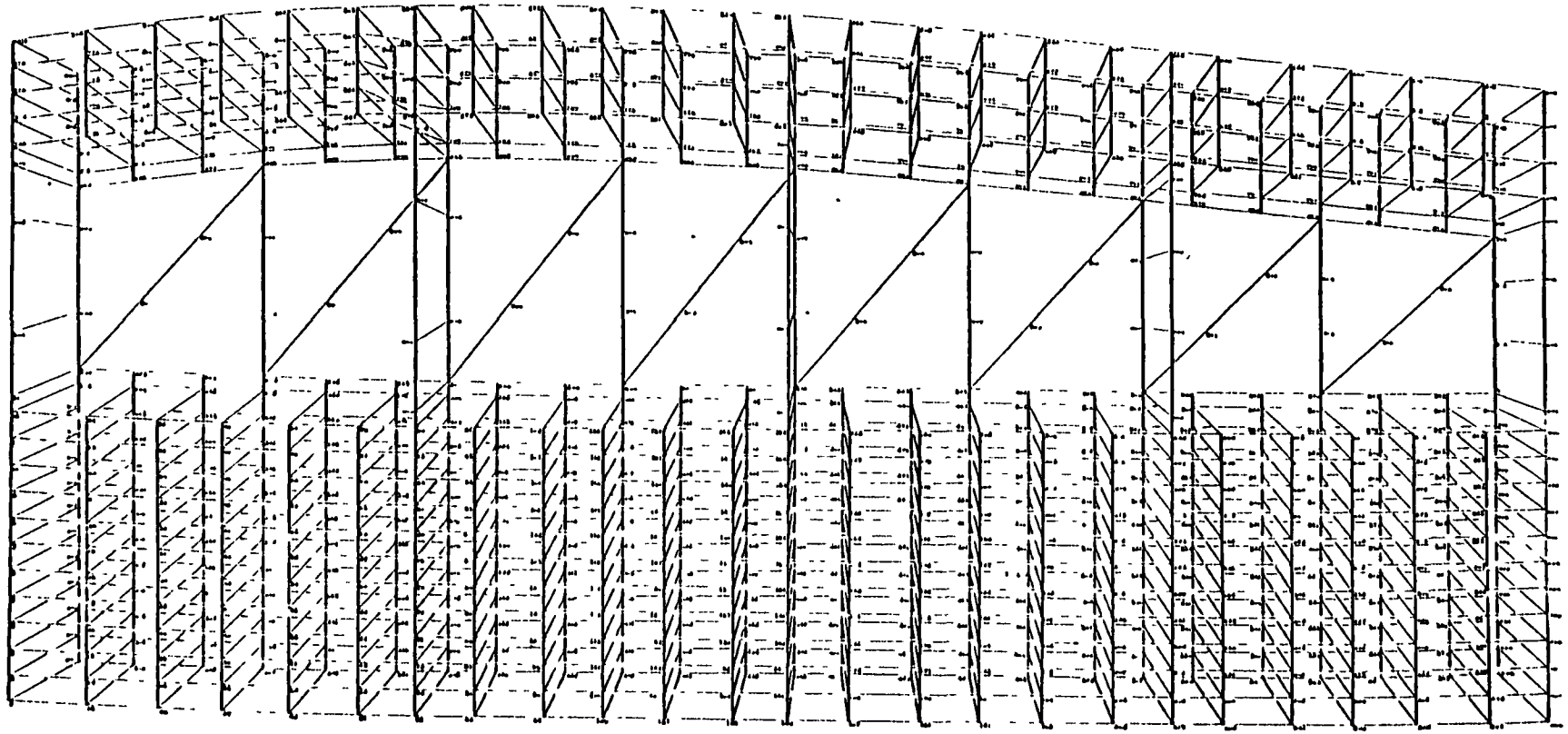

Figure 2. W.S. 240 Thermal Model

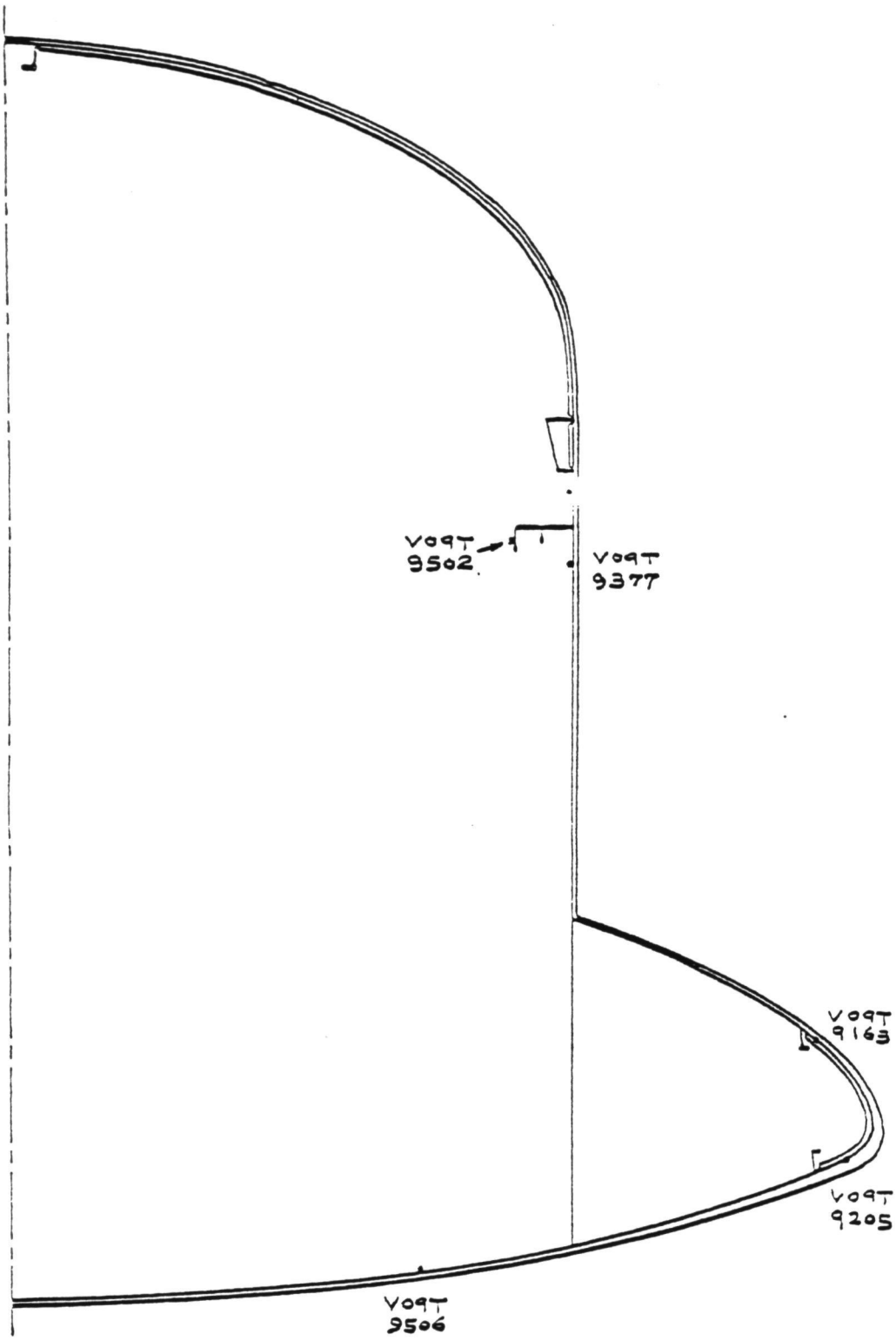

Figure 3. F.S. 877 Thermocouple Locations

Figure 4 - Flight Temperatures Compared to Predictions - Fuselage

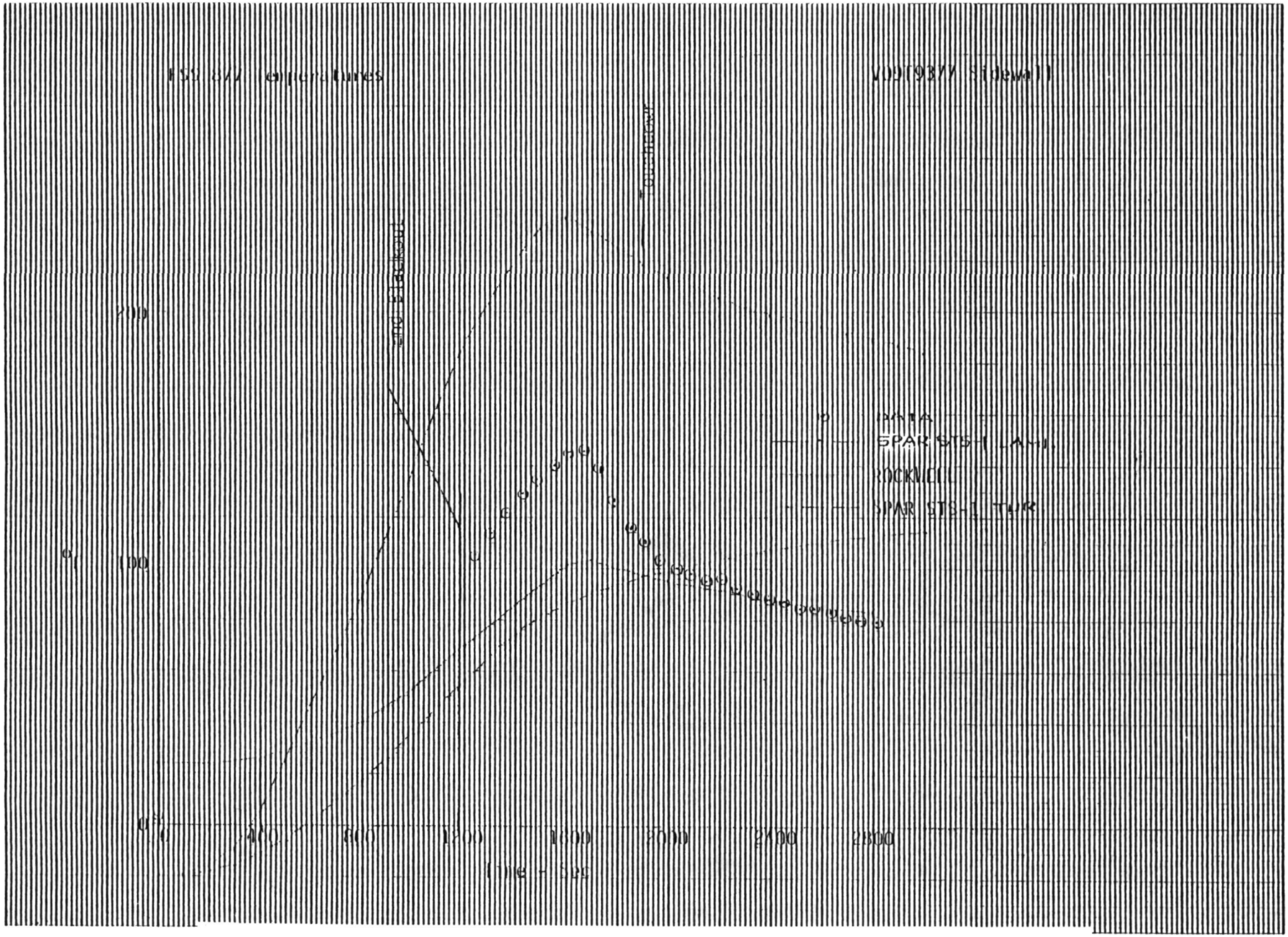

Figure 5 - Flight Temperatures Compared to Predictions - Fuselage

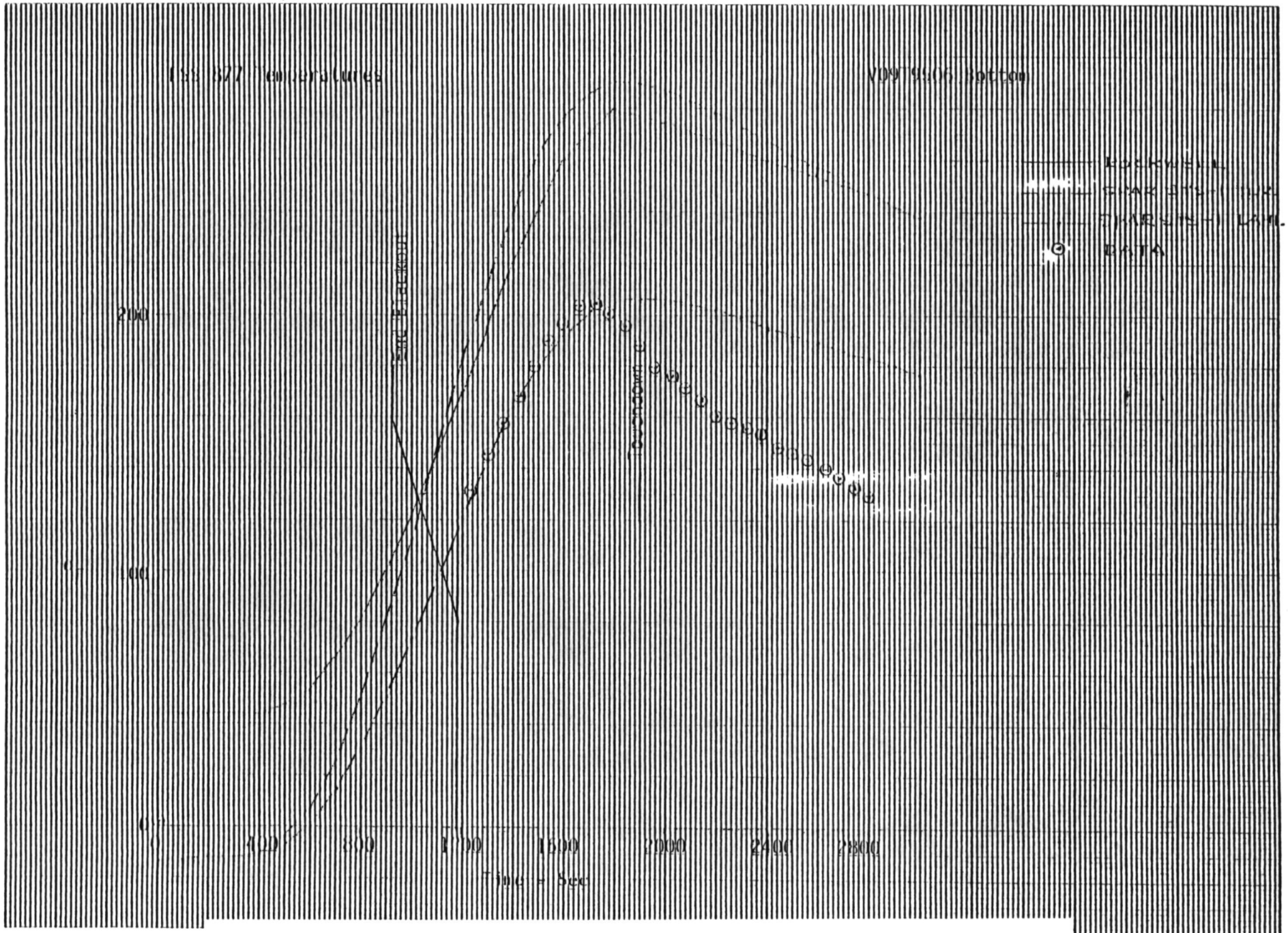

Figure 6 - Flight Temperatures Compared to Predictions - Fuselage

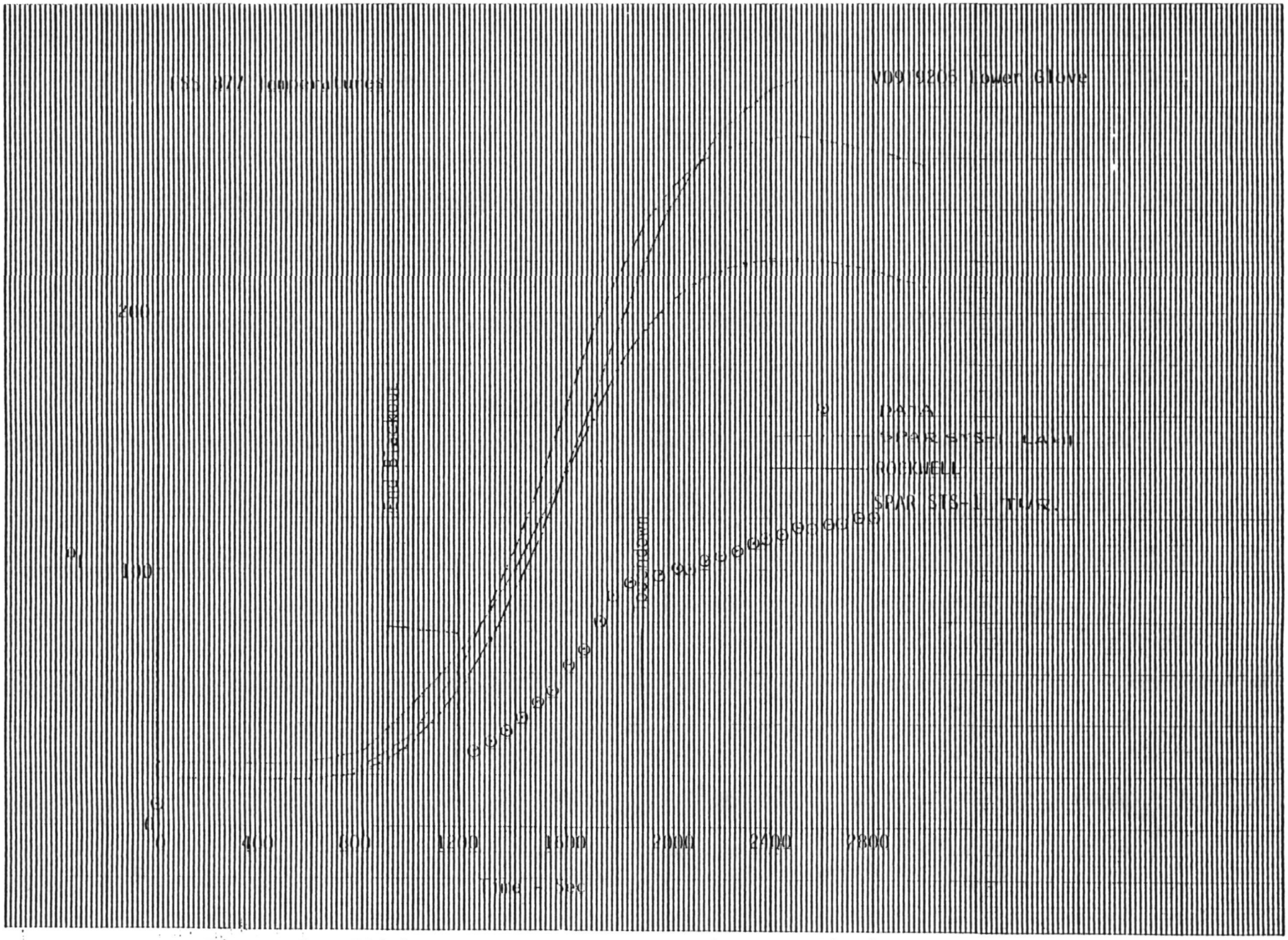

Figure 7 - Flight Temperatures Compared to Predictions - Fuselage

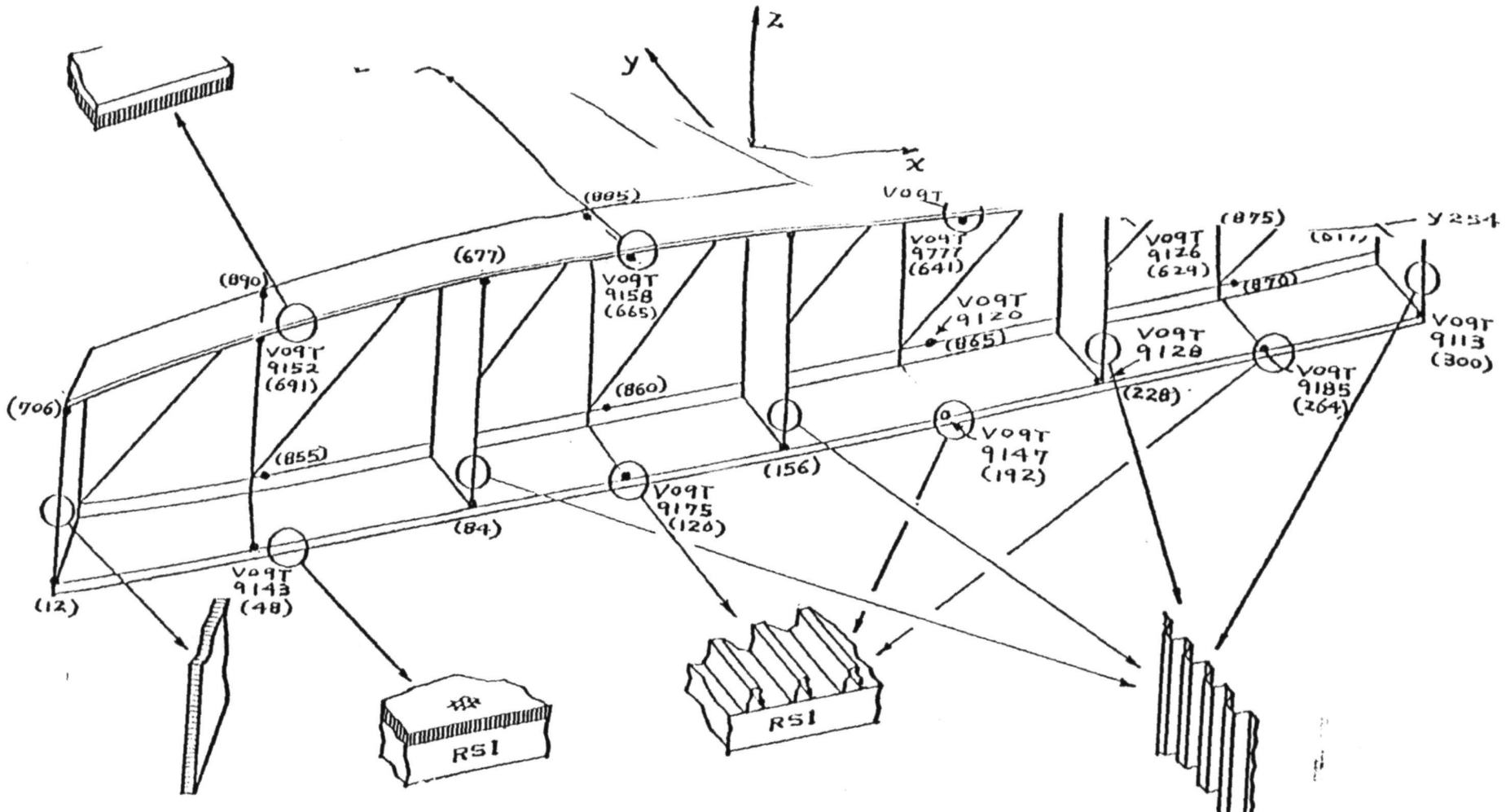

Figure 8. W.S. 240 Thermocouple Location

Figure 9 - Flight Temperatures Compared to Predictions - Wing

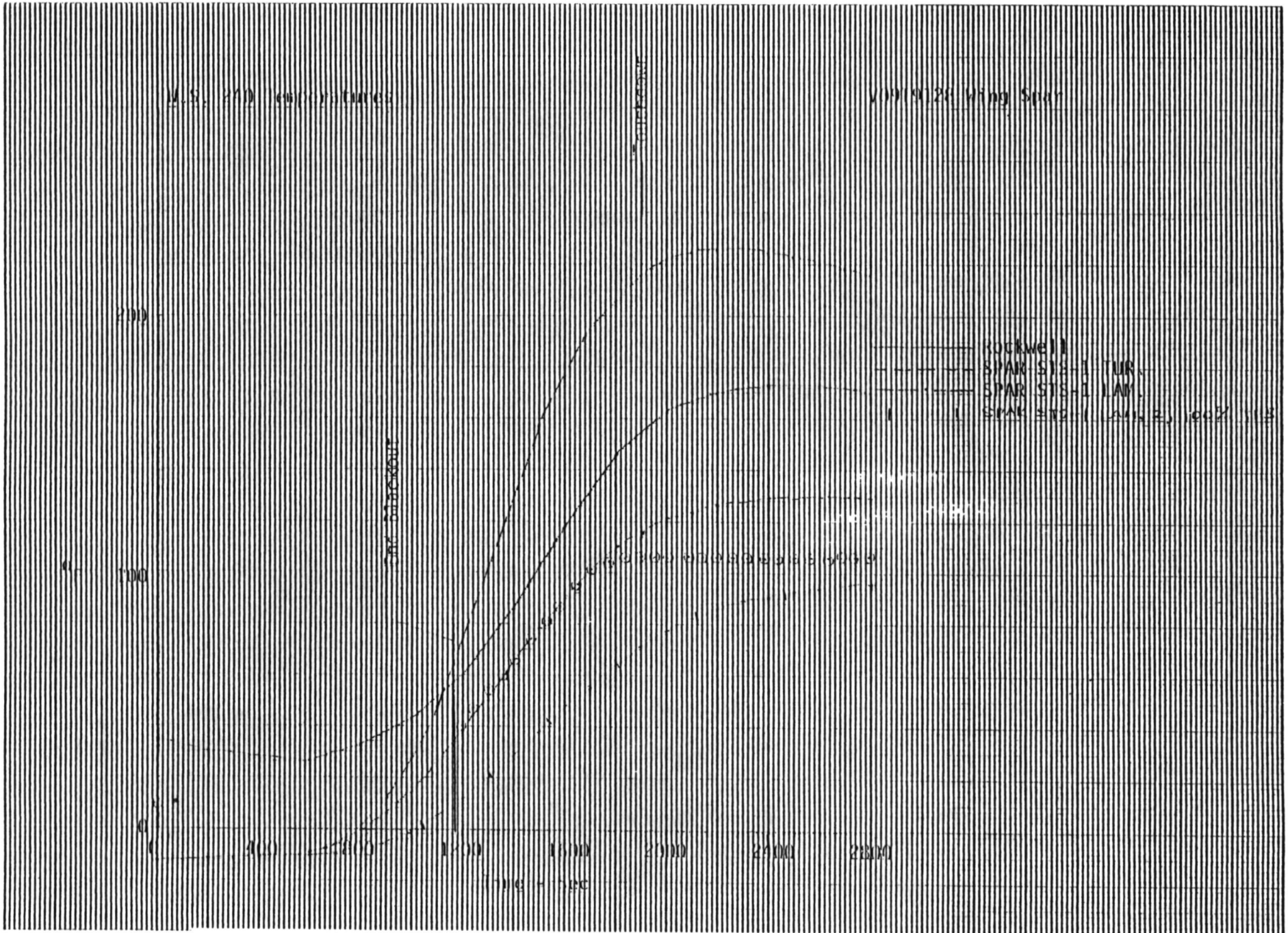

Figure 10 - Flight Temperatures Compared to Predictions - Wing

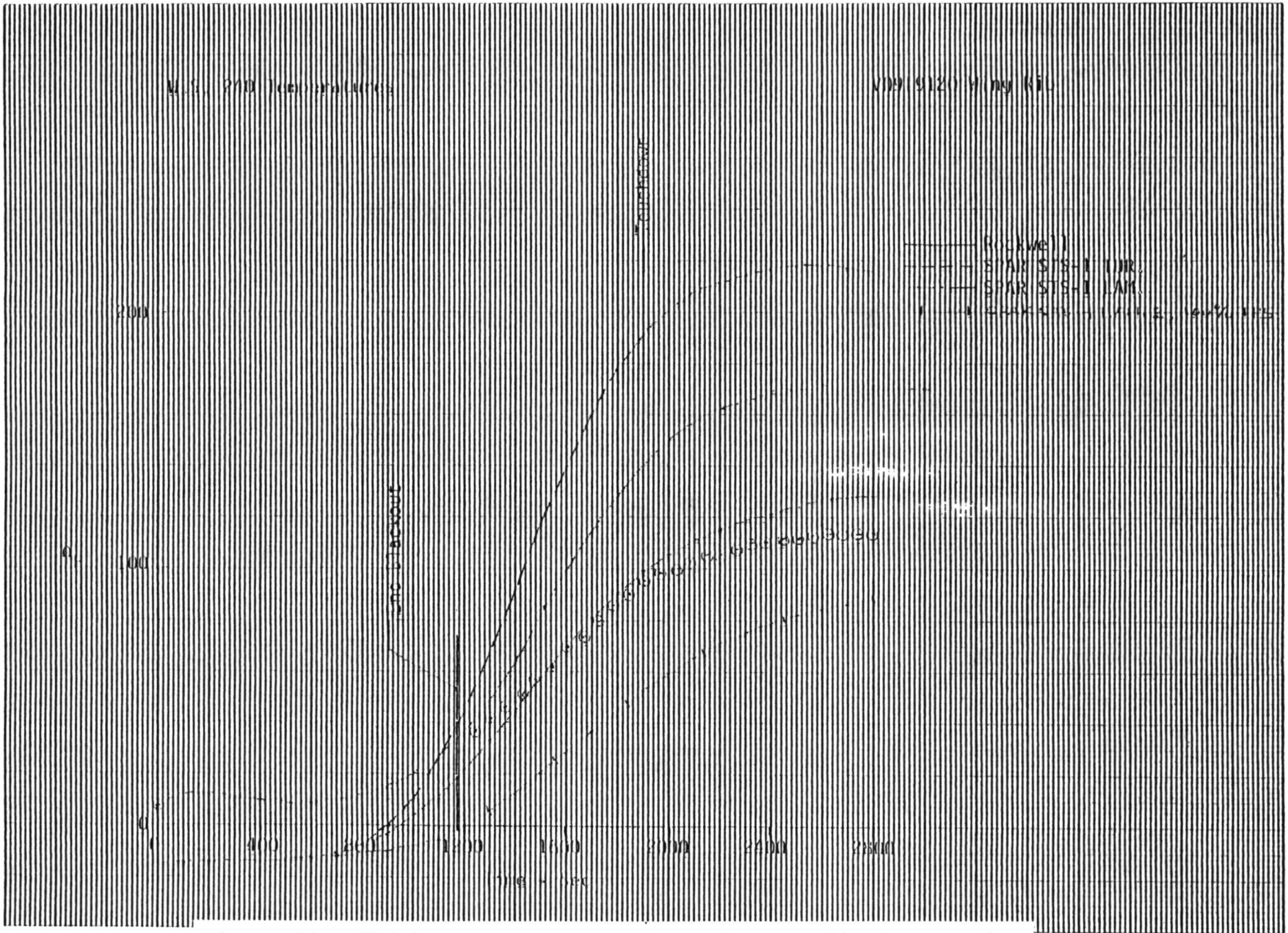

Figure 11 - Flight Temperatures Compared to Predictions - Wing

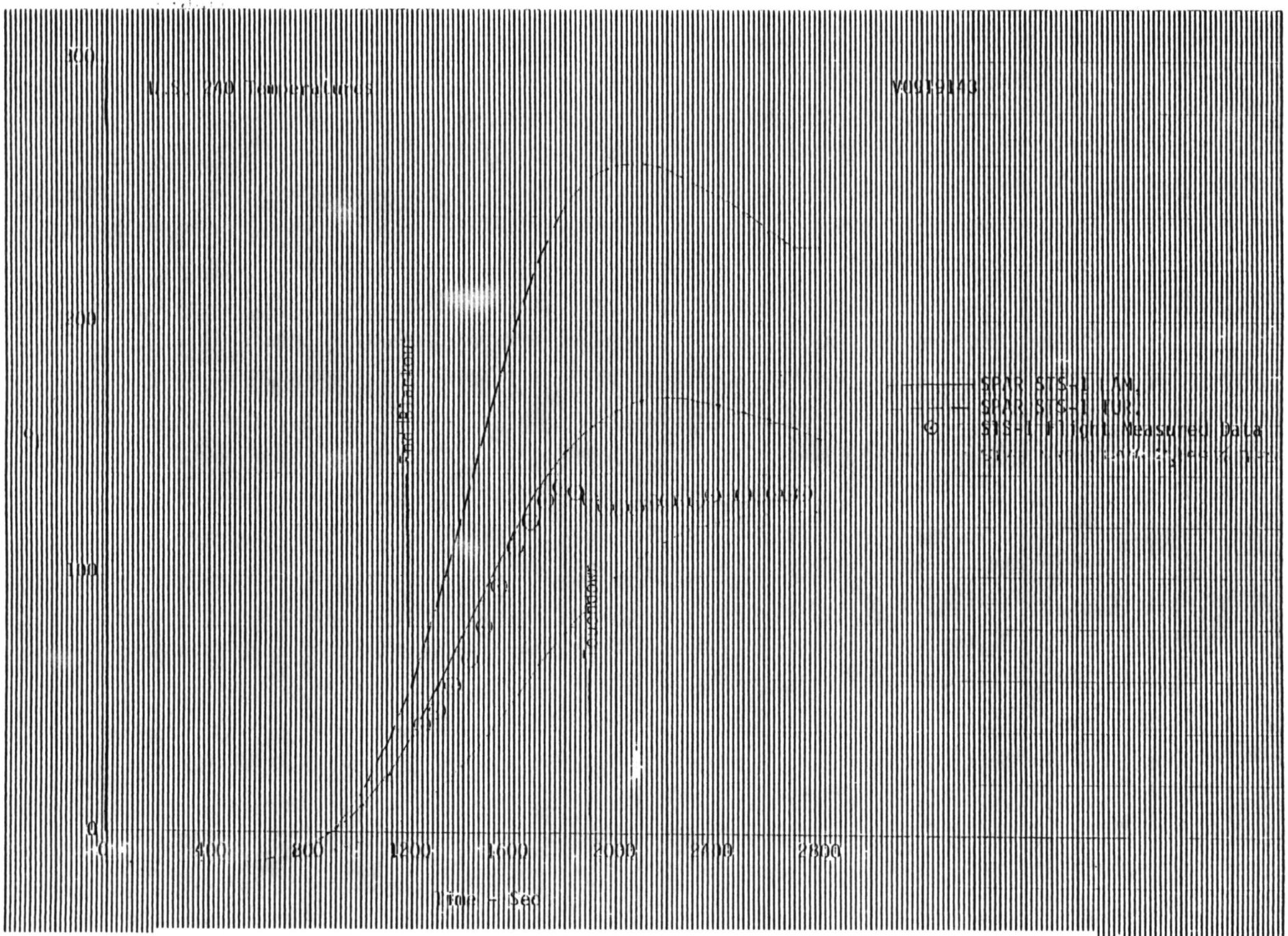

Figure 12 - Flight Temperatures Compared to Predictions - Lower Skin

Figure 13 - Flight Temperatures Compared to Predictions - Lower Skin

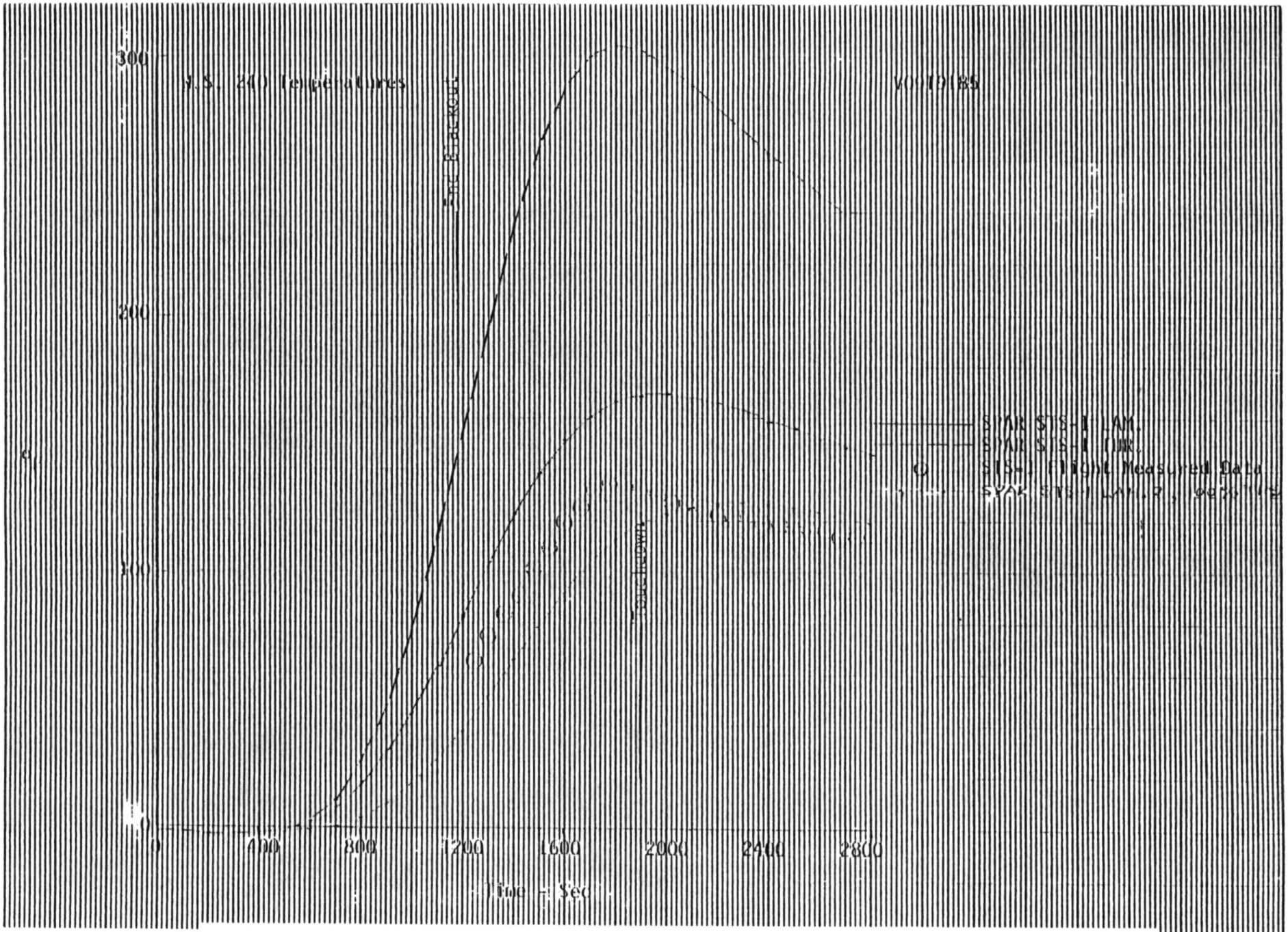

Figure 14 - Flight Temperatures Compared to Predictions - Lower Skin

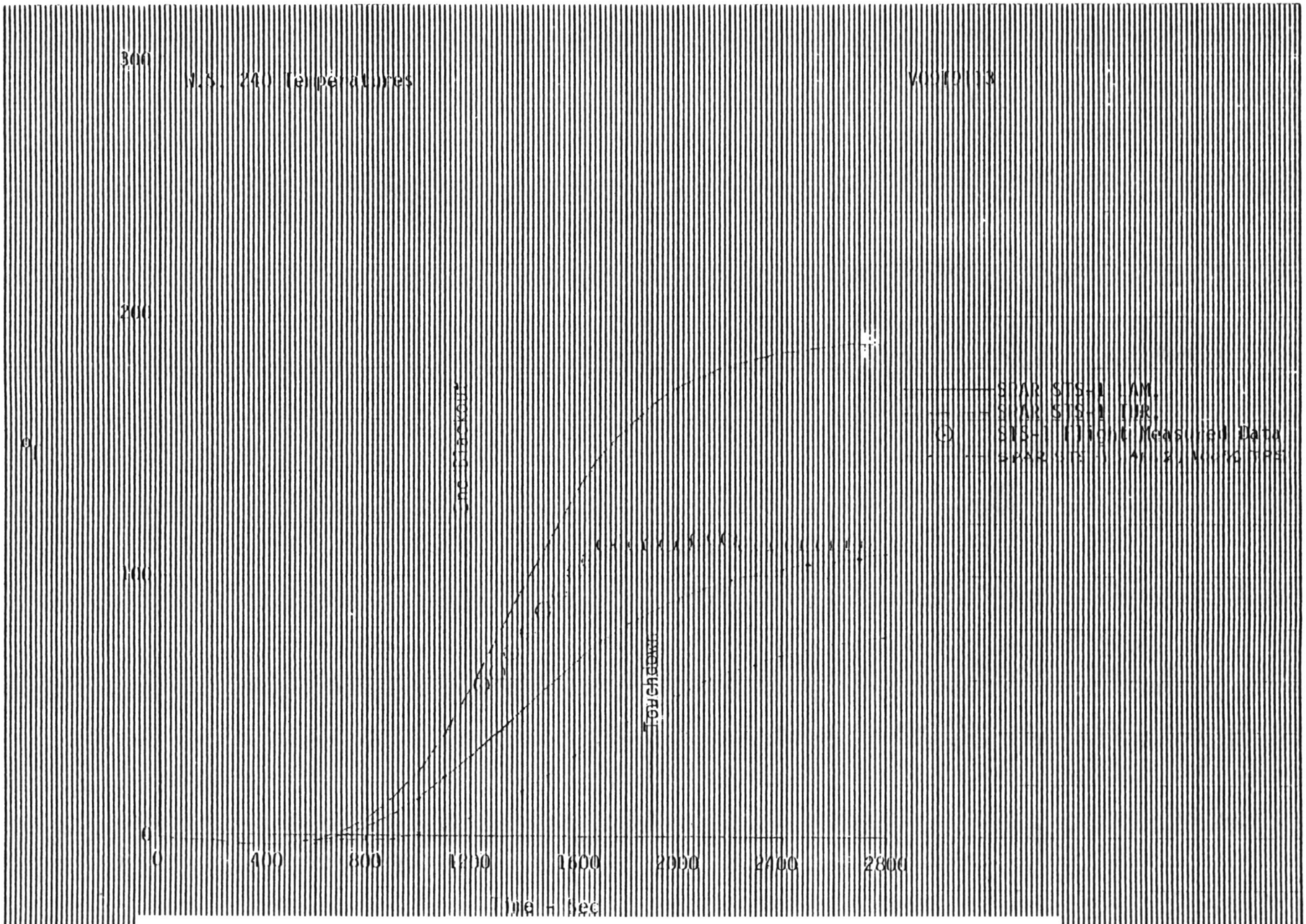

Figure 15 - Flight Temperatures Compared to Predictions - Rear Spar

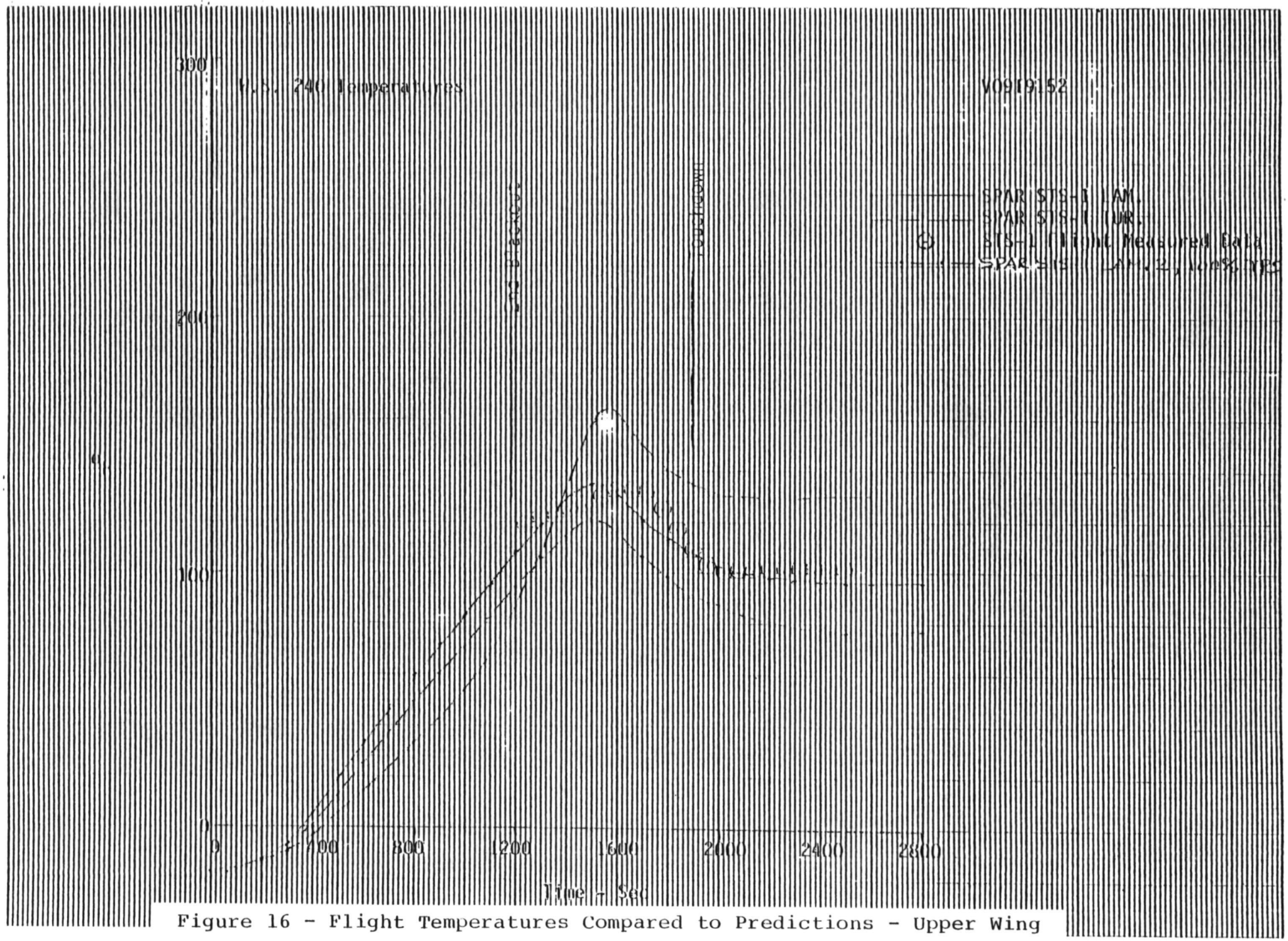

Figure 16 - Flight Temperatures Compared to Predictions - Upper Wing

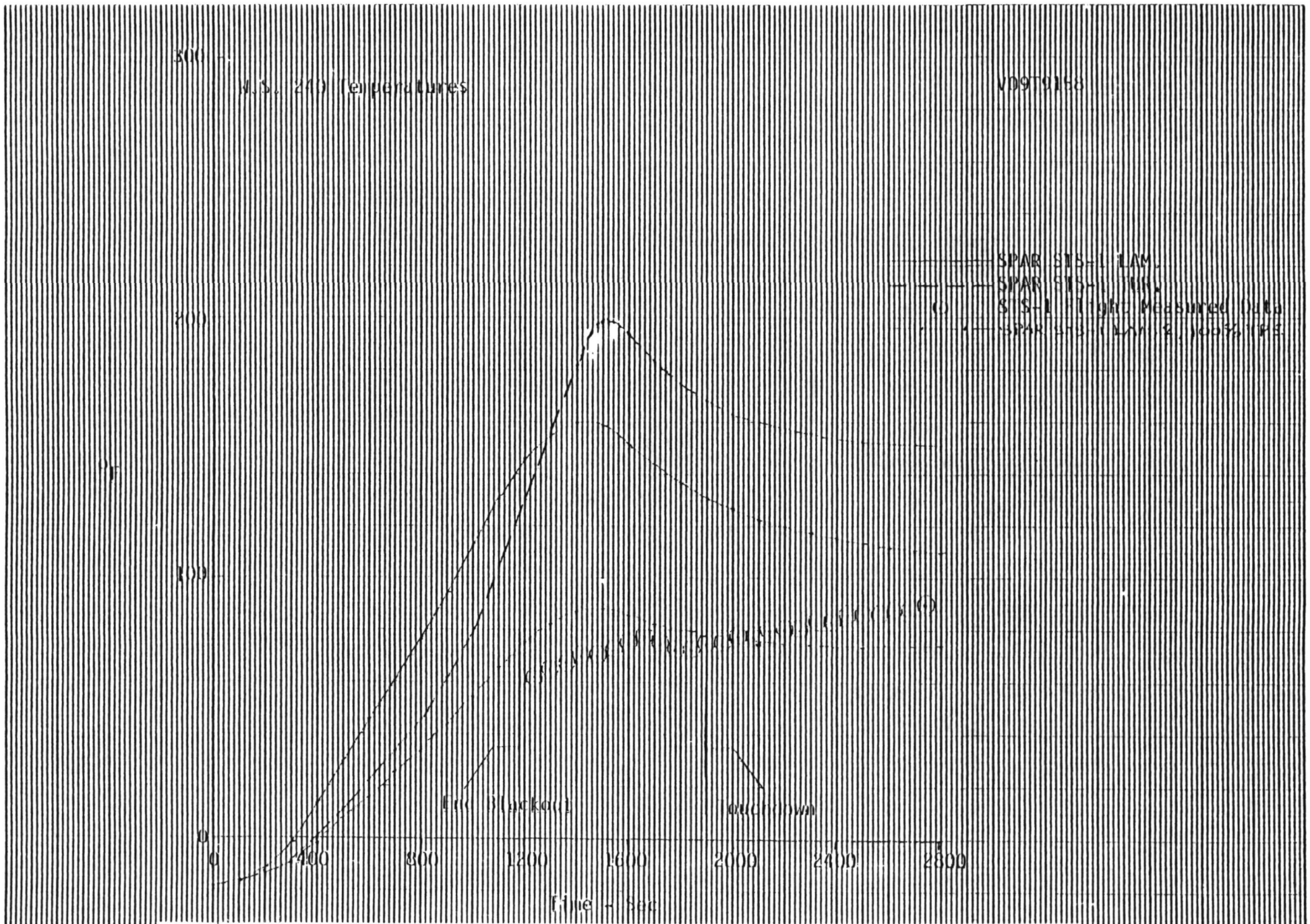

Figure 17 - Flight Temperatures Compared to Predictions - Upper Wing

Figure 18 - Flight Temperatures Compared to Predictions - Upper Wing

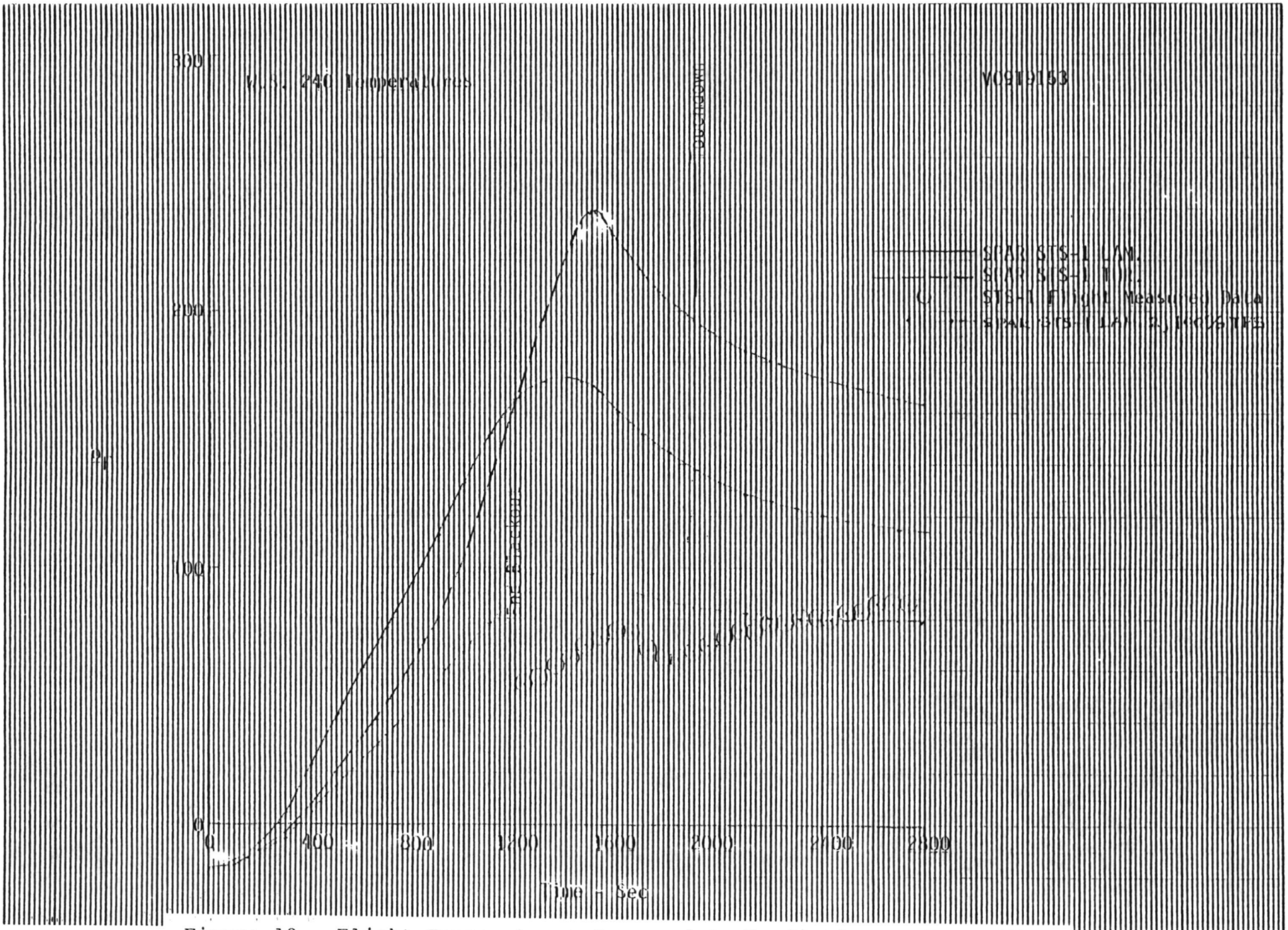

Figure 19 - Flight Temperatures Compared to Predictions - Upper Wing

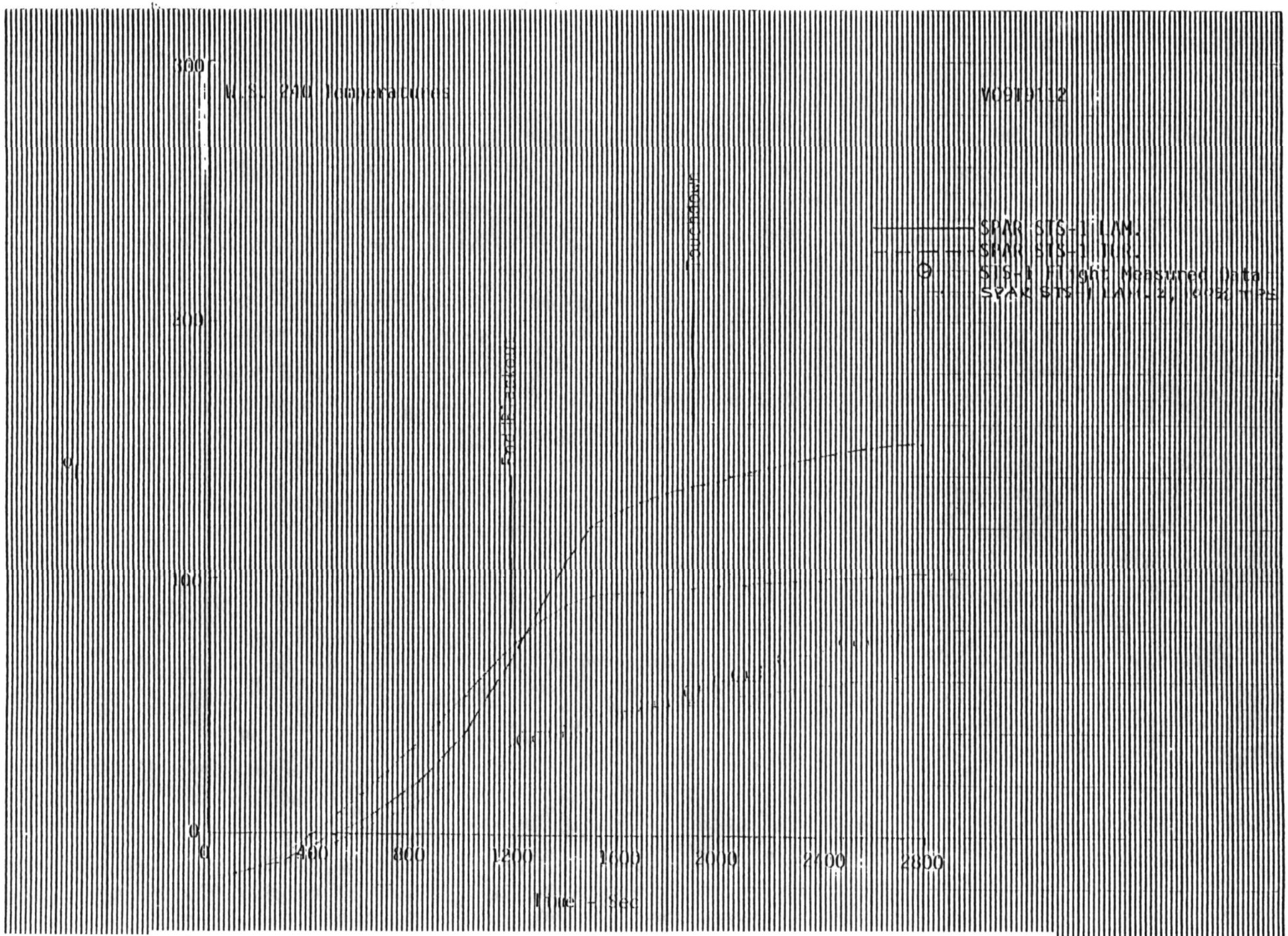

Figure 20 - Flight Temperatures Compared to Predictions - Upper Wing

Figure 21 - Flight Temperatures Compared to Predictions - Upper Wing

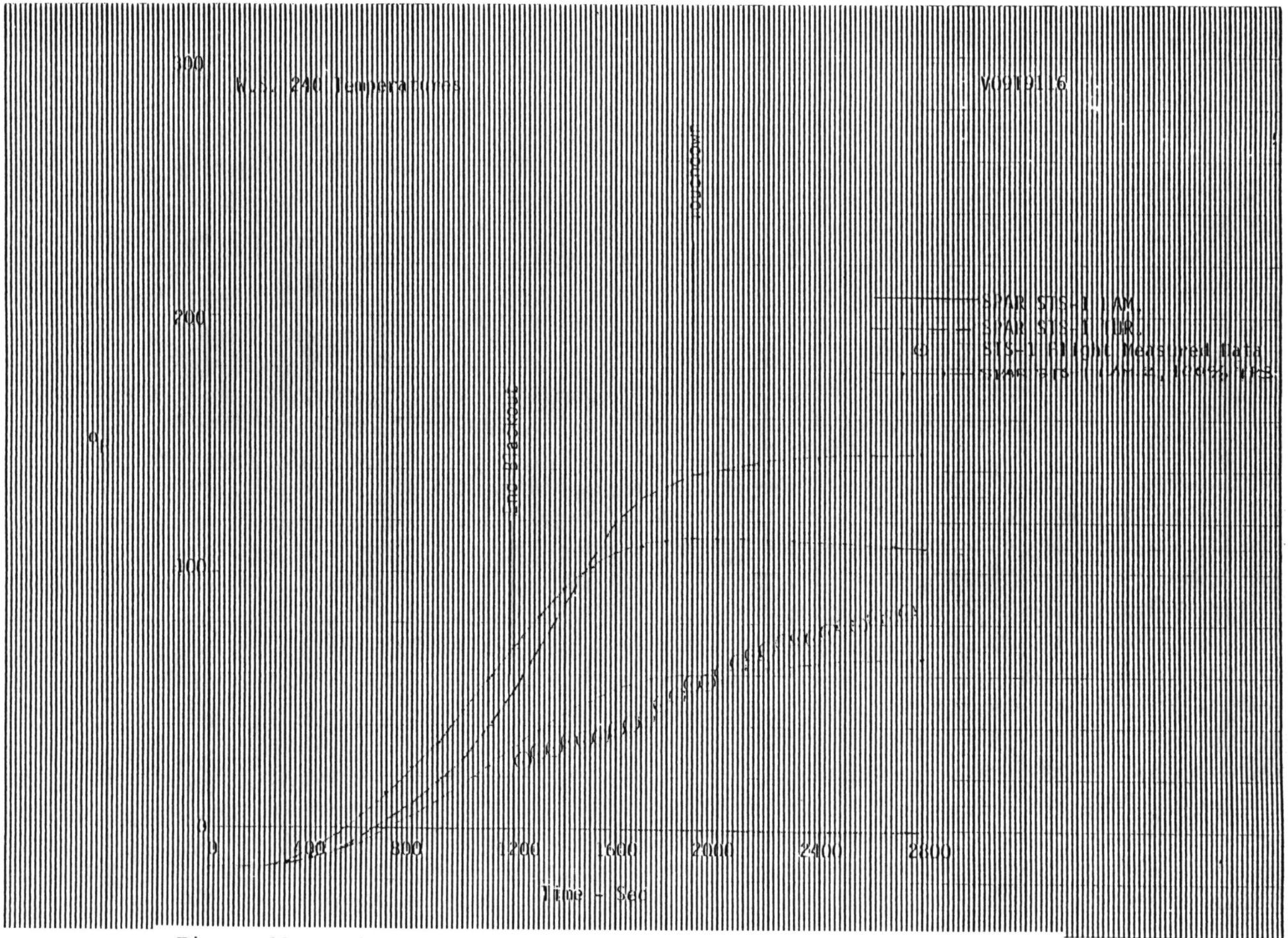

Figure 22 - Flight Temperatures Compared to Predictions - Upper Wing

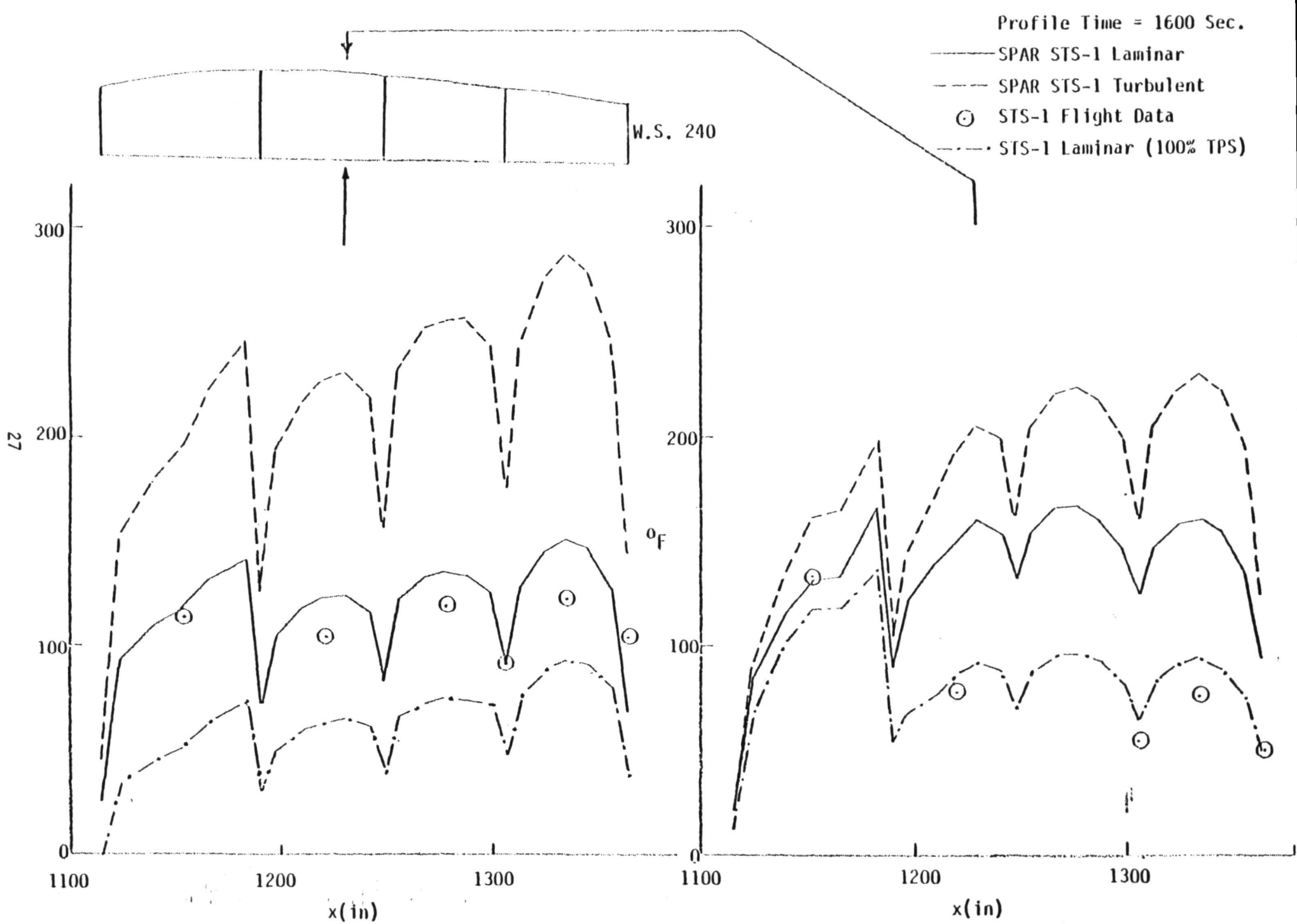

Figure 23. W.S. 240 Chordwise Temperature Distribution

Figure 24. Nominal vs Actual Trajectory Time History

SECTION II - PERFORMANCE, TRIM, AND CONTROL USE

Performance

Lift to drag ratios were determined during the entry from altitudes of approximately 272,800 feet to landing and Mach numbers from 24 to touchdown. The upper altitude limit was chosen because accelerometer readings above this altitude were too low to be acceptable for the transducer range. The flight lift to drag ratios were determined using the accelerometer method. For power-off conditions the following equation applies:

$$\frac{L}{D} = \frac{a_n \cos \alpha + a_\ell \sin \alpha}{a_n \sin \alpha \; a_\ell \cos \alpha}$$

where a_n and a_ℓ are the normal and longitudinal accelerations in g's, respectively, α is the angle of attack, and L/D is the lift to drag ratio. All the parameters needed for calculating and analyzing the flight and predicted lift to drag ratios were averaged over a 2 second time period using 25 sps data.

The lift to drag ratio as a function of Mach number is presented in figure 25. The flight and predicted values are essentially the same for Mach numbers from 5 to 24. Supersonically the largest disagreement occurs between Mach numbers of 1.8 and 4. In this Mach number range, the flight lift to drag ratio is as much as 7.5% lower than predicted. Below a Mach number of approximately 1, the flight and predicted lift to drag ratios have much larger variations. The maximum disagreements occur near a Mach number of 0.96, where the flight values are 22% lower than predicted, and near a Mach of 0.48, where the flight values are 27% higher than predicted. Near touchdown (Mach numbers less than 0.38), the flight lift to drag ratios vary from 15% higher to 2.5% lower than the predicted values.

The Mach number region below 1 is further examined in figure 26 as a composite time history of lift to drag ratio, elevon deflection, speed brake position, and Mach number. The time between 120 and 160 seconds corresponds to relatively stable elevon and speed brake positions; however, the increment between the flight and predicted lift to drag ratio is greater than for the immediately preceding and successive times, where these positions are changing. Because the elevon change is small and the speed brake change is large, the increment between the flight and predicted appears to be more affected by speed brake position than by elevon position.

The effect of speed brake position can also be seen in figure 27, where the lift to drag ratio near a Mach number of 0.6 is presented as a function of angle of attack for speed brake positions near 33° and 57°. The change in speed brake position from 33° to 57° corresponds to about a 0.5 change in the flight lift to drag ratio. The flight and predicted lift to drag ratios are in better agreement for the 57° speed brake position than for the 33° position.

Longitudinal Trim

The longitudinal trim characteristics are shown in figure 28. The elevator is driven to a scheduled value by the body flap and is generally within the body flap error deadband of the schedule except for speeds below 2000 ft/sec. The body flap position is shown in figure 28(b) along with the predicted value of body flap calculated from the flight observed surface positions and flight condition. Large errors in trim (up to 8 degrees) are seen above 10,000 ft/sec. This error corresponds to a pitching moment of $\Delta C_m = 0.02$ between 16,000 and 24,000 ft/sec.

Below 10,000 ft/sec there is good agreement between the flight and predicted body flap trim. In the 1500 to 2000 ft/sec. region, the elevator deviated about 2 degrees from its nominal schedule as a result of the body flap not being able to keep up with the changing trim requirement.

Lateral Trim

There was no evidence of any significant lateral trim required. Yaw jet firings were symmetric during the steady flight portion of the entry.

Control Use

Figure 29 shows the maximum control usage during the flight. Rudder, aileron, and elevator use is low compared to that available. The body flap is near its maximum capability in both directions in several parts of the entry. This is of no concern from a controllability standpoint since elevator capability is sufficient for pitch control. Pitch and roll jets never exceed two jets firing simultaneously during the entry. The yaw jet use is about one-half the maximum capability down to the turn at M = 18. This turn and the one at M = 9 require full yaw jet capability. The M = 5 and M = 3 turns require short periods of maximum yaw jet use, and this could possibly be alleviated by using more of the rudder capability.

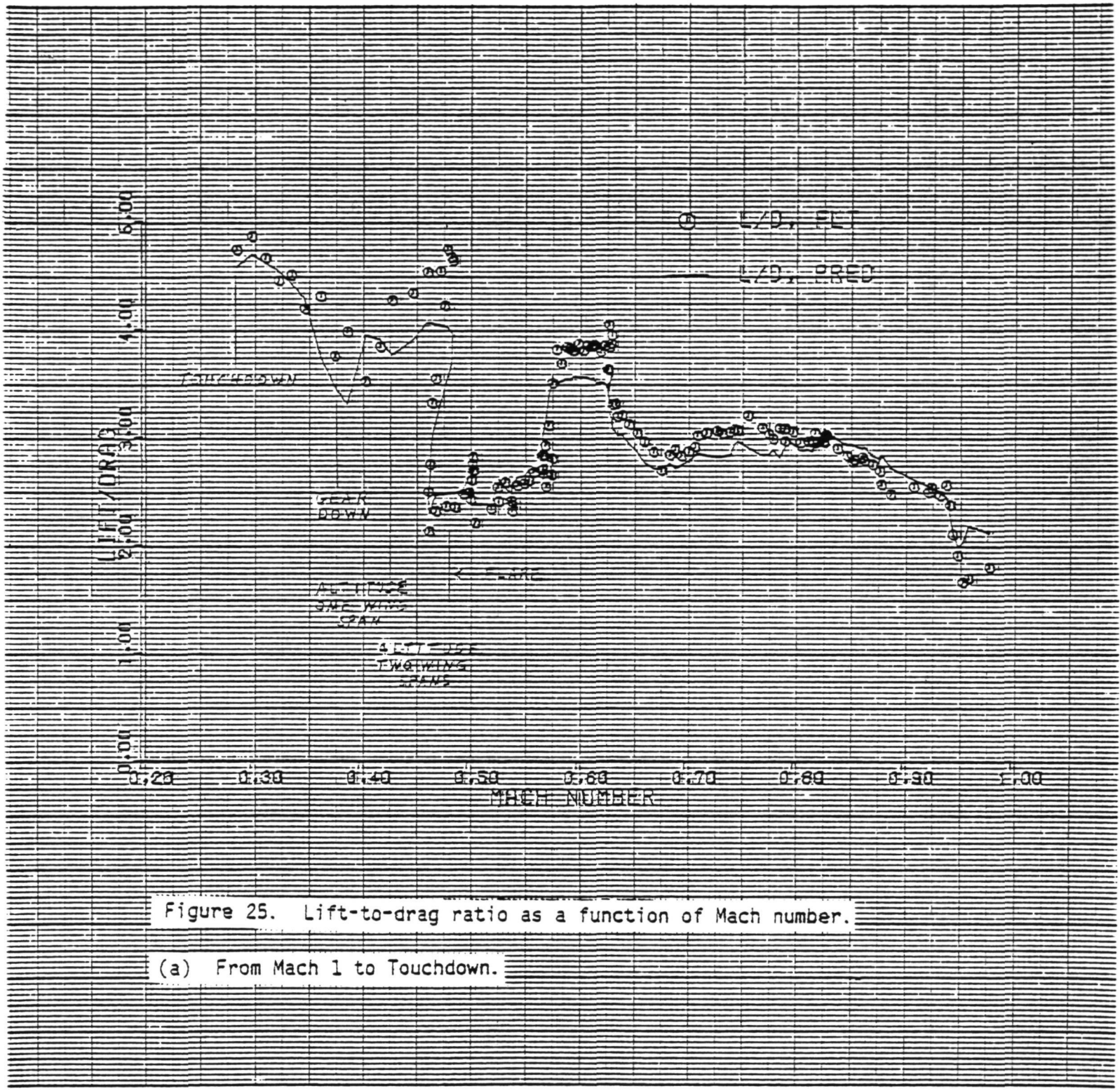

Figure 25. Lift-to-drag ratio as a function of Mach number.

(a) From Mach 1 to Touchdown.

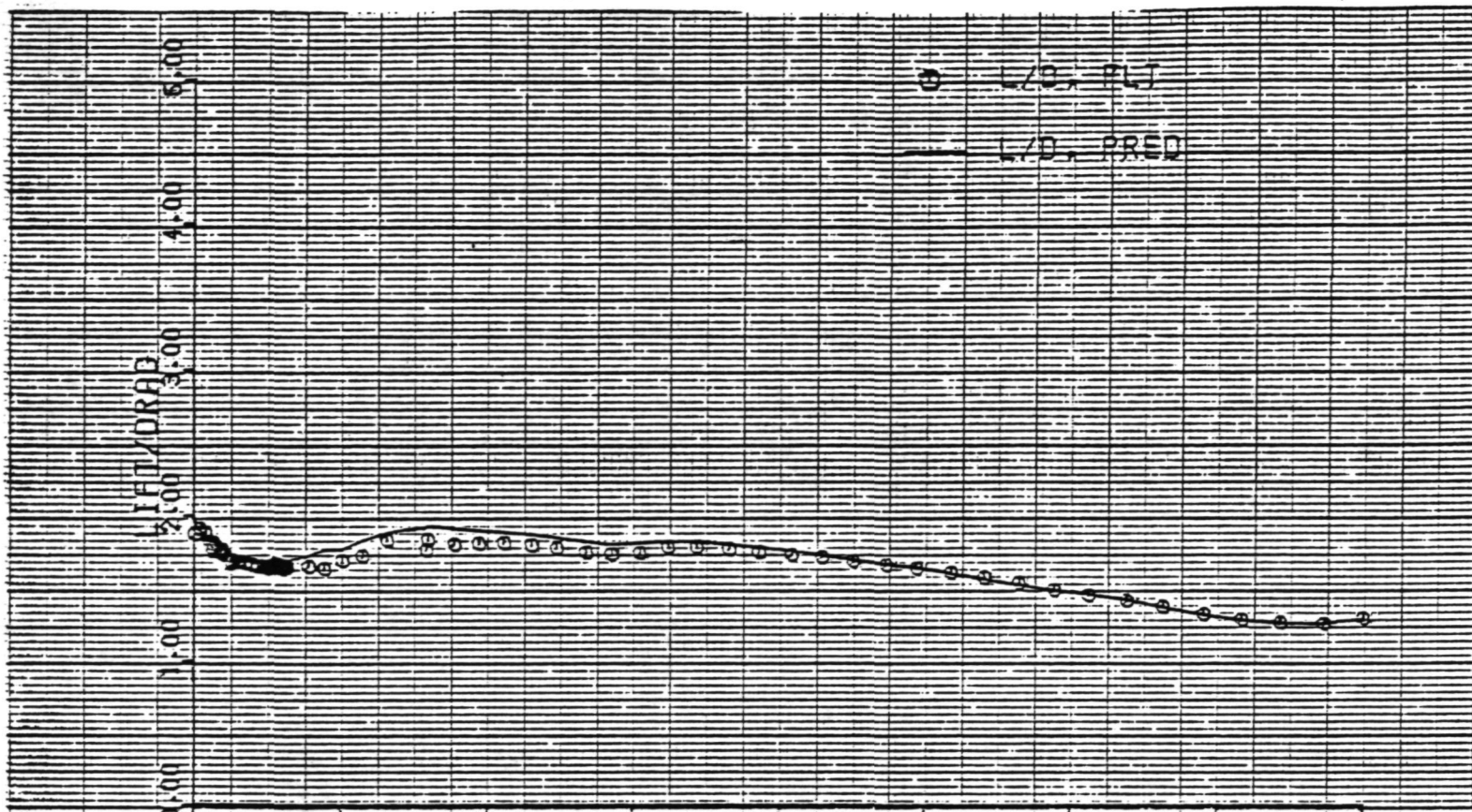

(b) From Mach 9 to 1.

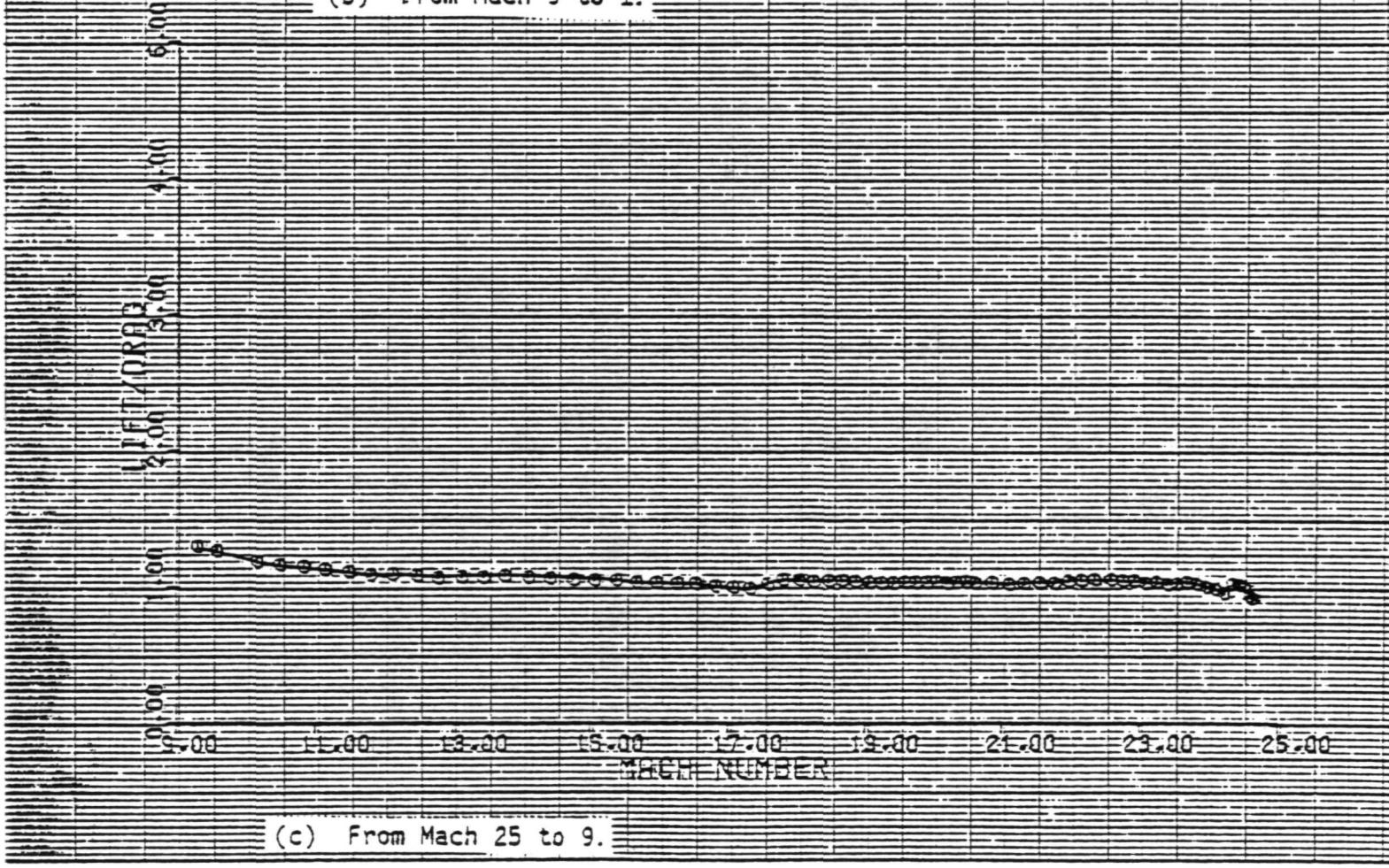

(c) From Mach 25 to 9.

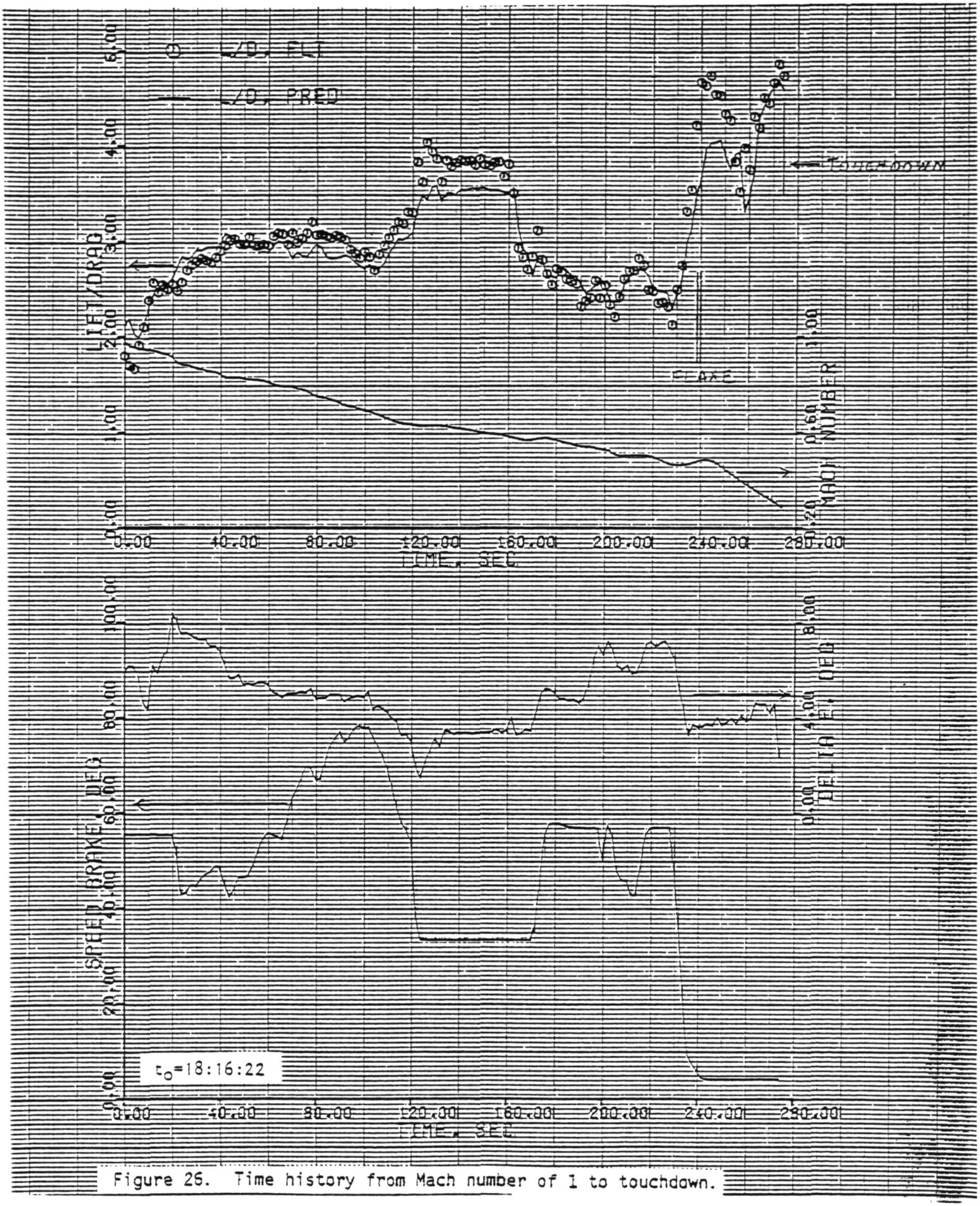

Figure 25. Time history from Mach number of 1 to touchdown.

$.55 \leq M \leq .64$
$10900\,ft \leq h \leq 25400\,ft$

PRED	FLT	ELEVON DEFLECTION	SPEED BRAKE
- - -	●	1.5° to 3.2°	33°
	○	3.3° to 4.1°	
———	■	3.0° to 3.9°	57°
	□	4.7° to 5.2°	

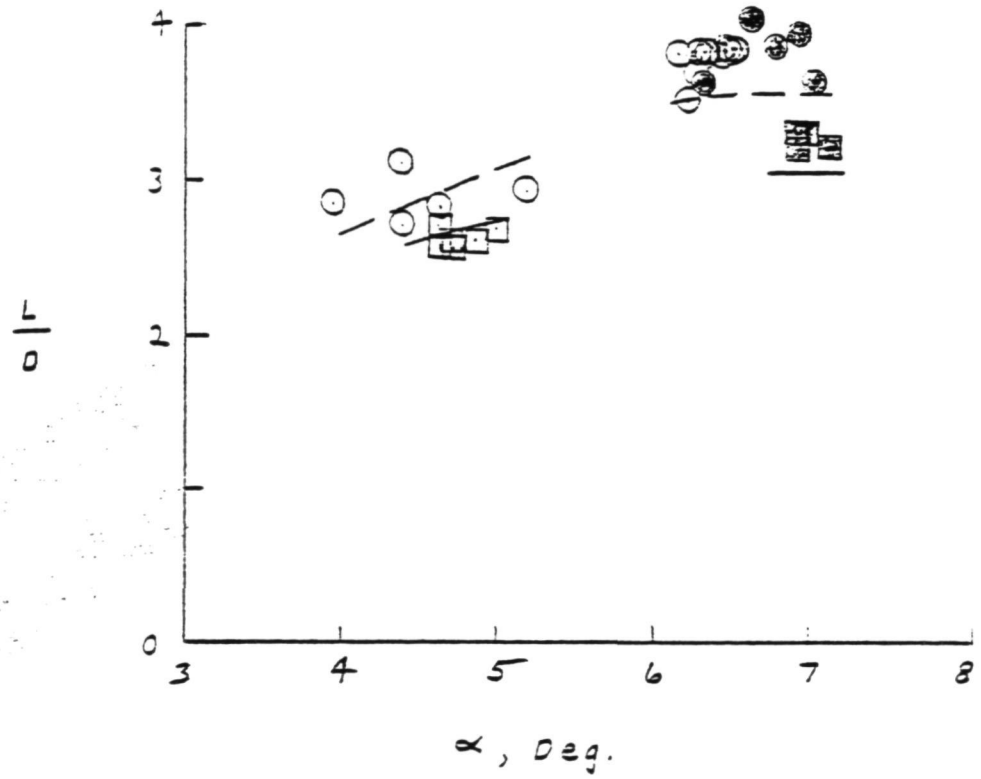

Figure 27. Effect of speed brake deflection on L/D.

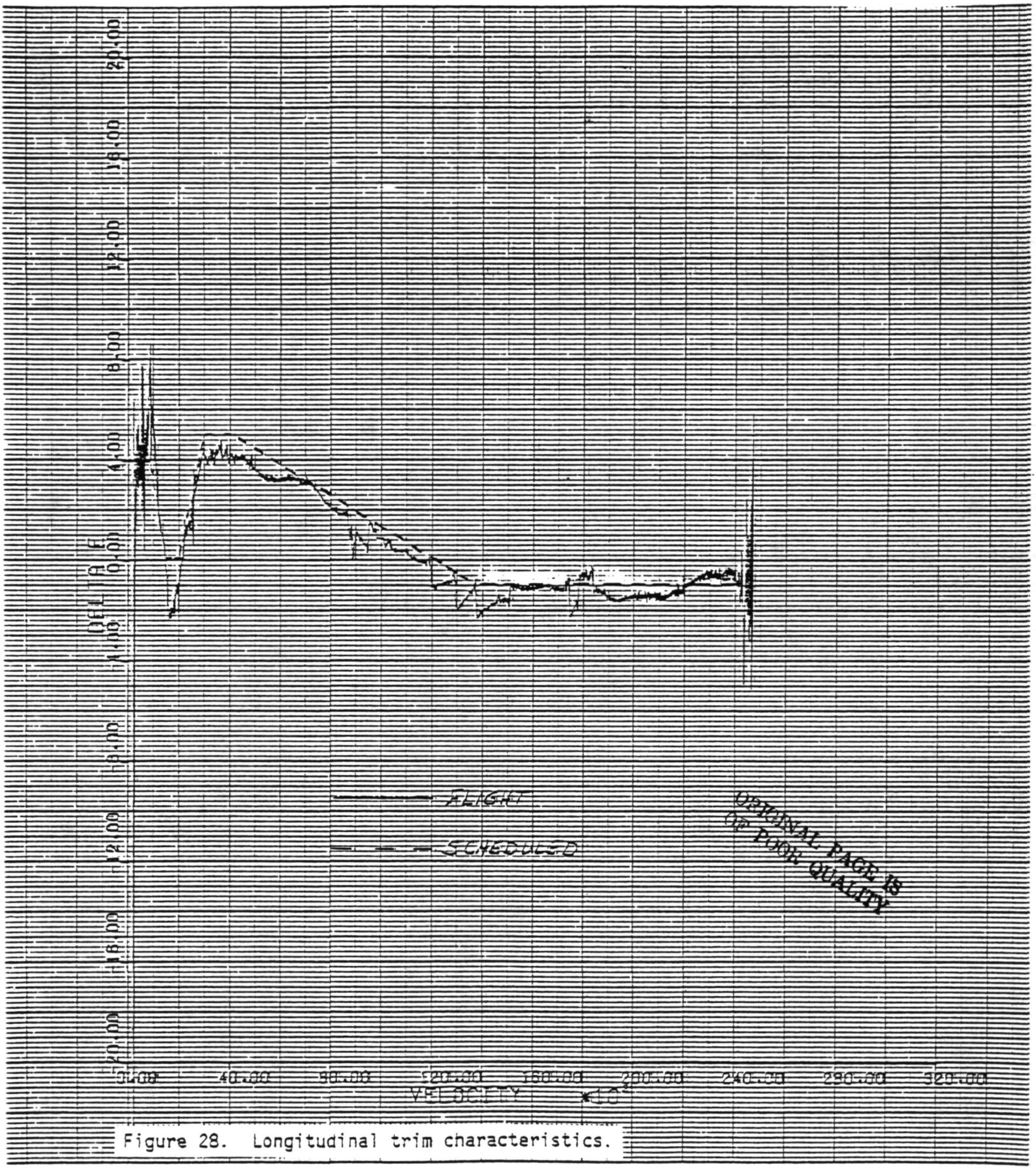

Figure 28. Longitudinal trim characteristics.

(a) Elevator.

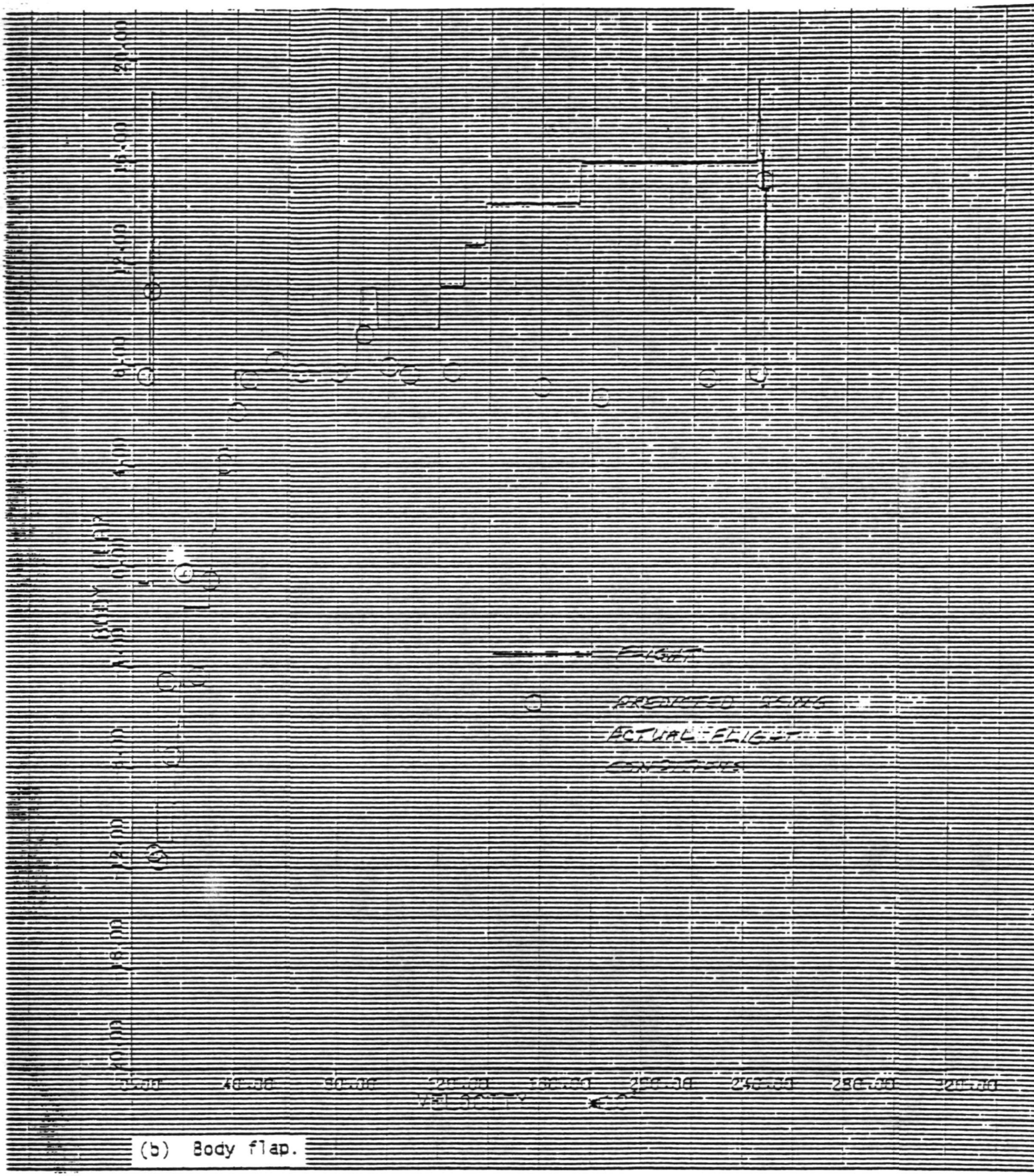

(b) Body flap.

Figure 28. Concluded.

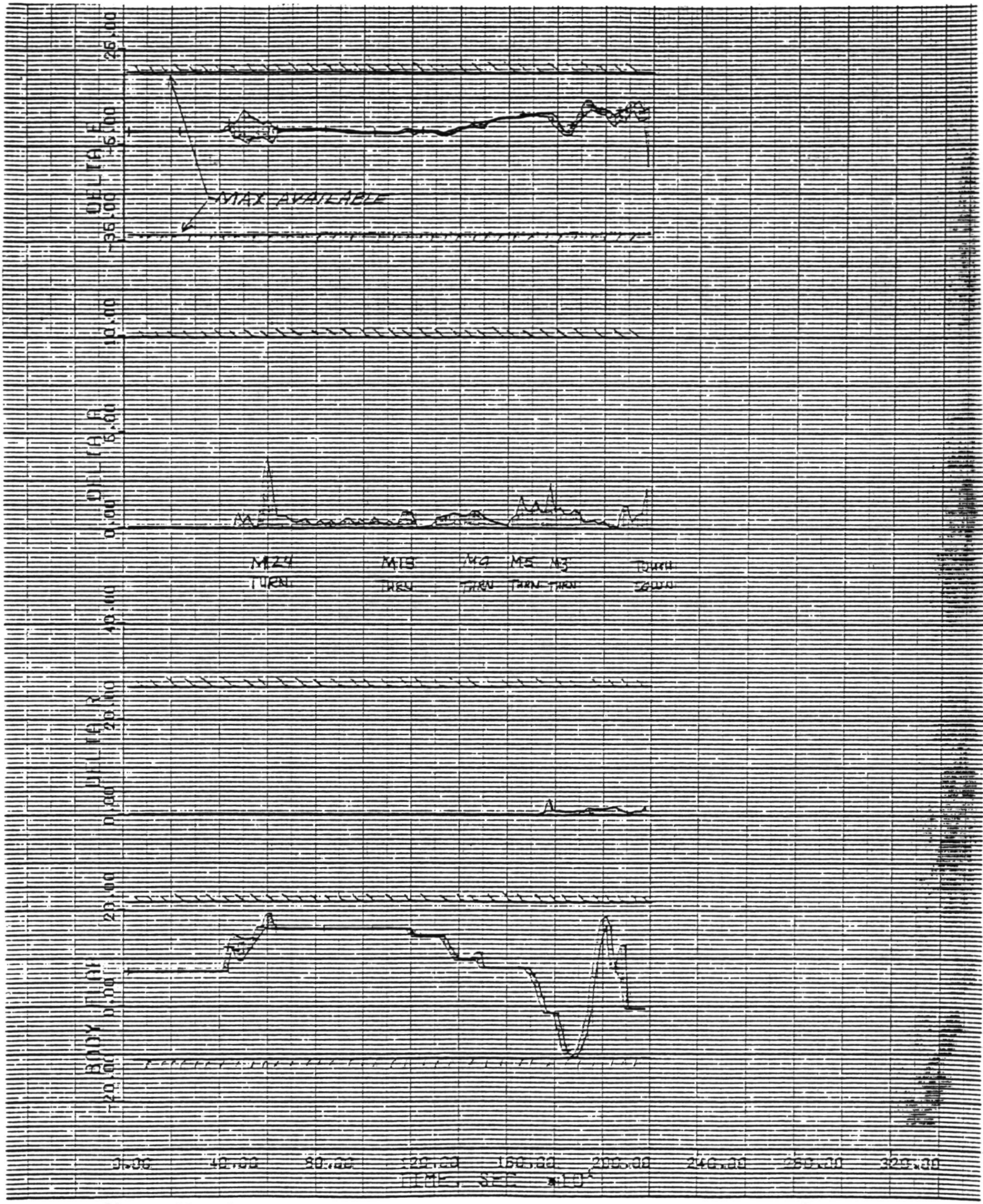

Figure 29. Control use during entry. Minimum/maximum or absolute values calculated for 20 second intervals.

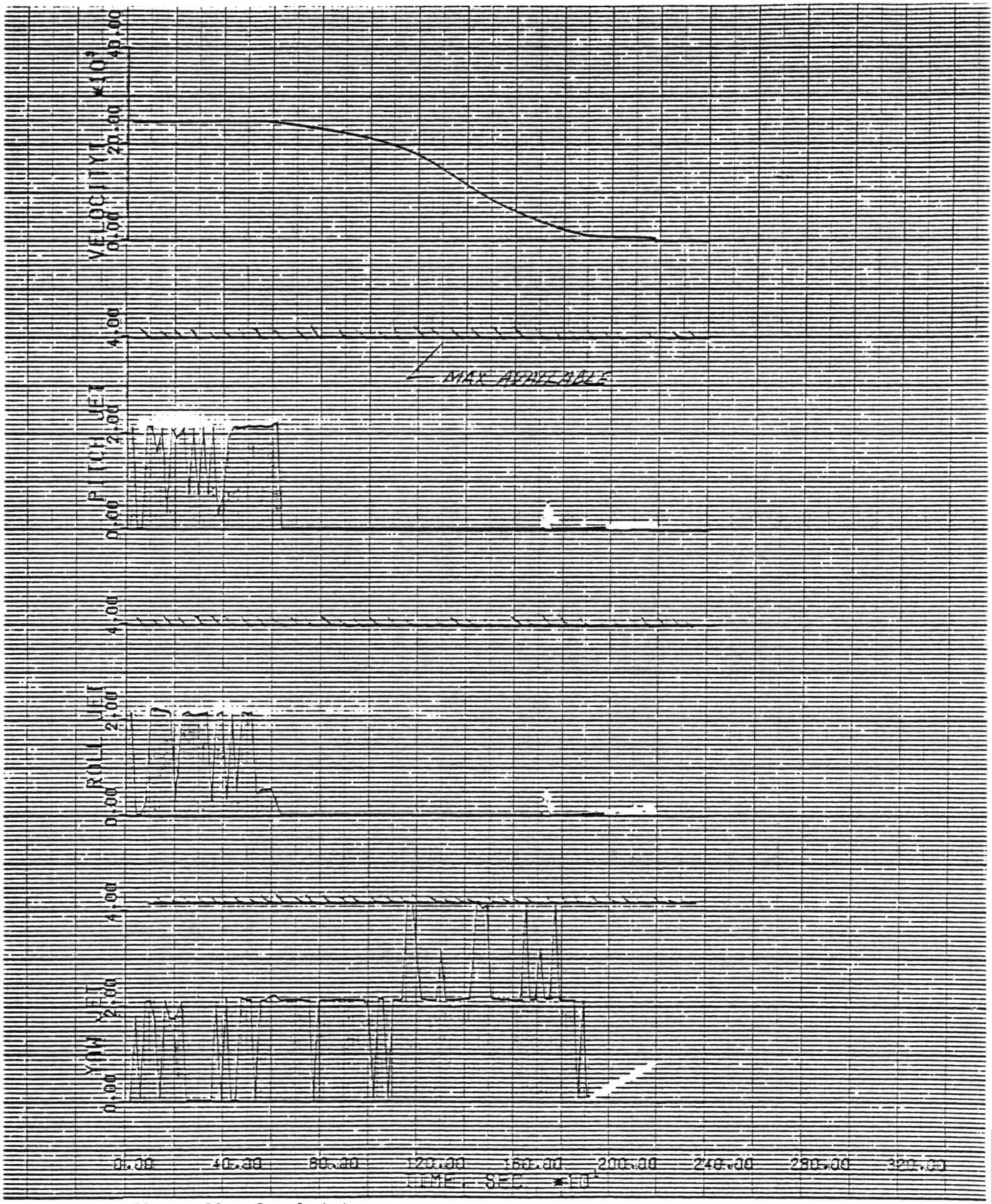

Figure 29. Concluded.

SECTION III - PRELIMINARY STABILITY AND CONTROL ANALYSIS FOR STS-1

The flight data from STS-1 include unique and very interesting information on aircraft flight dynamics. Maneuvering manned flight was demonstrated for the first time over a wide range of hypersonic velocities. These data have provided the opportunity to assess flight characteristics in completely new regimes. Among the flight characteristics to be assessed are the stability and control derivatives estimated from normal maneuvering flight on STS-1.

Estimates of the stability and control derivatives can be used in flight envelope expansion, to update simulators, to enhance maneuvering capability and flying qualities and to provide the information necessary to improve flight control systems. After the analysis of the flight test data, the estimated derivatives can be compared with calculated and wind tunnel predictions, and this comparison can be used to update prediction methods for the improvement of future aircraft design.

Today the primary method of obtaining estimated derivatives from flight data is the maximum likelihood estimates (ref. 1) or the output error method. The results for STS-1 were obtained from the maximum likelihood estimation program, MMLE-3 (ref. 2). The estimation problem can be defined in general terms. The system investigated, in this case the shuttle spacecraft, is assumed to be modeled by a set of dynamic equations containing unknown stability and control derivatives. To determine the values of the unknown derivatives the system needs to be excited by a suitable control input (either from the pilot or programmed test inputs). The input and the spacecraft response are both measured. In the case of the shuttle the primary source of these measurements is the ACIP package, although data from the OI and GPC systems were also used. The values of the derivatives are then inferred based on the requirement that the model response to a given input match the actual aircraft measured response. The mathematical formulation of the technique used in the following analysis is contained in reference 3. Some of the practical implications of applying the MMLE-3 program to flight data are contained in references 4 and 5.

Analysis of the STS-1 data used many maneuvers that were not designed specifically for derivative extraction. These maneuvers, although far from ideal for high quality derivative extraction, did provide some valuable information on the spacecraft stability and control derivatives. The maneuvers of most value were the planned bank reversals. Even these maneuvers were designed to produce very little in the way of dynamic response. Therefore where bank reversals were performed, only fair derivative estimates should be expected. The quality of the maneuvers for stability and control derivative estimation were less desirable below a Mach number of 3.5 because of several additional factors. The feedback to the rudder surfaces begins in this region. Although the highest quality derivative estimates are obtained with no feedback, it has been demonstrated that useful estimates can be obtained if independent control inputs are made, that is, inputs independent of the feedback signals. If no such independent inputs are available, a condition of near linear independence (ref. 4) is encountered, usually resulting in misleading or

unreasonable estimates. This, of course, results in the program (or algorithm) being unable to distinguish accurately between the effect of the control motions (control derivatives) and the effect of the feedback response variables (rotary derivatives). The match between the flight data and the computed response may be excellent, but the derivatives themselves may be unreasonable. The STS-1 data were difficult to analyze in a meaningful way below a Mach number of 3.5 because there were no independent rudder inputs below this Mach number and very few independent pilot aileron inputs. Therefore the only results considered valid and presented in this paper at Mach numbers of less than 3.5 are those where an independent aileron input was made. A discussion of the difficulties encountered in the analysis of the other "maneuvers" is found later in this section.

Additional difficulties were also found below a Mach number of 1.8, when a mild transonic buffet was evident. A stronger buffet between a Mach number of 0.8 and 1.0 made the analysis even more difficult. The primary method of analyzing data in strong buffet is to assume that state noise is present in the system model (refs. 2 to 5). The additional state noise assumption for the model for maneuvers in buffet will be used where independent control motions are present; however, to date this analysis has not been attempted on the shuttle data.

Another problem in the data occurs because the only sideslip measurement is from the inertial system. Therefore, in a wind shear or in turbulence the sideslip measurement is in error. There are two possible solutions to the problem: 1) use the state noise assumption for the model and estimate the wind shear or turbulence along with the derivatives; or 2) reconstruct sideslip angle to account for the shear or turbulence. One way the second solution can be approached is to use the side probe measurements to obtain an independent estimate of sideslip angle. This approach is currently being attempted, but no substantive results are available at this time.

In summary, the data suitable for derivative extraction below a Mach number of 3.5 are exceedingly limited, for the following reasons: 1) no independent rudder motions exist, 2) aerodynamic buffet is considerable, and 3) the sideslip measurement is contaminated with wind shear or turbulence.

Since the last two sources of data contamination will probably remain in succeeding flights, it is even more important for specific maneuvers to be accomplished on the next flight in order to obtain accurate derivatives in this Mach number region.

Longitudinal Stability and Control Derivatives

The only longitudinal stability and control characteristics that have been examined are for Mach numbers above 18. Very few of the longitudinal maneuvers at the lower Mach numbers can be used for derivative extraction, but derivative extraction will be attempted in the future

using these data. There were only a small number of small amplitude maneuvers above a Mach number of 18, so the flight estimates are not very accurate. Among the more important derivatives, C_{m_α} was estimated to an accuracy of about 20%, $C_{m_{\delta_e}}$ to 15%, $C_{m_{BF}}$ to 40%, and pitch jet moments to 10%. The estimates obtained to date give no basis for revising any of the data book values. The data book predictions all fall within the fairly large accuracy bands of the derivative estimates. Further assessment will require additional and more suitable maneuvers for longitudinal stability and control derivative estimation.

Lateral-Directional Stability and Control Derivatives

The derivative estimates obtained to date are shown in figures 30 and 31. The derivative estimates are plotted as a function of Mach number. The symbol is the derivative estimate and the vertical bars are the uncertainty bounds (refs. 4 and 5). The poorer the estimate, the larger the uncertainty bounds. The dashed line is a fairing of the flight-determined derivative estimates, and the solid line is the Aero Data Book (Aerodynamic Design Data Book, Rockwell report number SD72-SH-0060) value for the derivative at the same flight conditions as the flight maneuvers were obtained. The solid ticked lines are a ±1 variation applied to the Aero Data Book values. The square symbols indicate maneuvers where $|\beta| < 1.5°$ and $|\delta_a| < 2°$, and the circle indicates maneuvers where $|\beta| < 4°$ and $|\delta_a| < 4°$. The shaded symbol indicates that $q \cong 0$. All of the derivatives presented are per degree except for the derivatives due to yaw jet firings. The side force due to yaw jet is in pounds, and the rolling and yawing moments are in foot-pounds. The Mach number range is from 1.8 to 24.5.

The reason the sets of values for β and δ_a are separated is that there may be some nonlinearities in these variables as a function of the state and control variables . The maneuver at a Mach of 24.5 was split into two segments, inasmuch as the value of C_{n_β} and $C_{n_{\delta_a}}$ appear to be different in the two segments. Since the shuttle will probably fly in the future within the bounds of the lower range of β and δ_a, the flight fairing goes through these points. It still remains to decide how best to represent this nonlinearity.

In general the derivatives are in fairly good agreement with the Aero Data Book values. C_{y_β} (fig. 30(a)) from flight is smaller in magnitude than the data book value between Mach numbers of 1.8 and 5 and between Mach numbers of 18 and 25. C_{ℓ_β} (fig. 30(b)) is in good agreement with the data book values up to a Mach number of 18, above which the flight value is of smaller magnitude than the prediction. The flight values for C_{n_β} (fig. 30(c)) show a more rapid trend toward increasing stability as Mach

number decreases than the predictions and are outside the ±1 variation bounds near Mach 4. $C_{y_{\delta_a}}$ (fig. 30(d)) from flight is somewhat larger than predicted. $C_{n_{\delta_a}}$ (fig. 30(e)) shows good agreement between flight and data book. $C_{\ell_{\delta_a}}$ (fig. 30(f)) is in good agreement, although the flight data show a somewhat smaller value between Mach 5 and 10, where the values fall near the ±1 variation bounds. Flight and prediction for Y_{YJ} (fig. 31(a)) and N_{YJ} (fig. 31(c)) are in good agreement throughout the Mach number range. The most notable discrepancy between the flight data and the data book values for L_{YJ} (fig. 31(b)) is above a Mach number of 10, where the sign is the opposite of that predicted.

The rudder derivatives are not presented because of the near linear dependence problem mentioned previously. Many attempts at analysis were made to try to find reasonable estimates for these maneuvers. Since the rudder and rotary derivatives are affected by near linear dependence, a wide variety of rudder derivatives were obtained for a wide range of rotary derivatives. In addition, multiple minima were encountered when the elements of the weighting matrix were also determined during the analysis. A wind shear is obviously present during all maneuvers below a Mach number of 1.8. Based on experience of analyzing aircraft stability and control derivatives on over 40 different aircraft configurations, the two most difficult derivatives to estimate from even high quality stability and control maneuvers are L_{δ_r} and L_r. Therefore, because of near linear dependence problems for the rudder derivatives, multiple minima problems, wind shears, and very marginal maneuvers, we feel that one can only be misled by placing any value in the results of analyzing maneuvers obtained in this region of the first flight. The problems can only be solved by independent rudder and aileron inputs in this region on future shuttle missions. Any other approach is apt to put unrealistic and undesirable restrictions on all future shuttle missions.

Comments

The highly successful STS-1 flight demonstrated the technical soundness of the space shuttle concept. The few problems encountered have been addressed, and in most cases solutions have been found. The criticism of the maneuvers from STS-1 is not a criticism of the flight or its objectives; the primary concern on that mission was to return the shuttle safely from space. However, as future flights are planned, it must be remembered that if the full utility of the vehicle is to be realized, it will be necessary to further define the stability and control characteristics. If the large uncertainties that currently exist in these characteristics are not removed, the vehicle will be restricted as to the center of gravity and trajectories it can fly. The only way to improve our understanding of the vehicle's characteristics is by performing intentional stability and control maneuvers with independent control motions either through PTI's or pilot inputs.

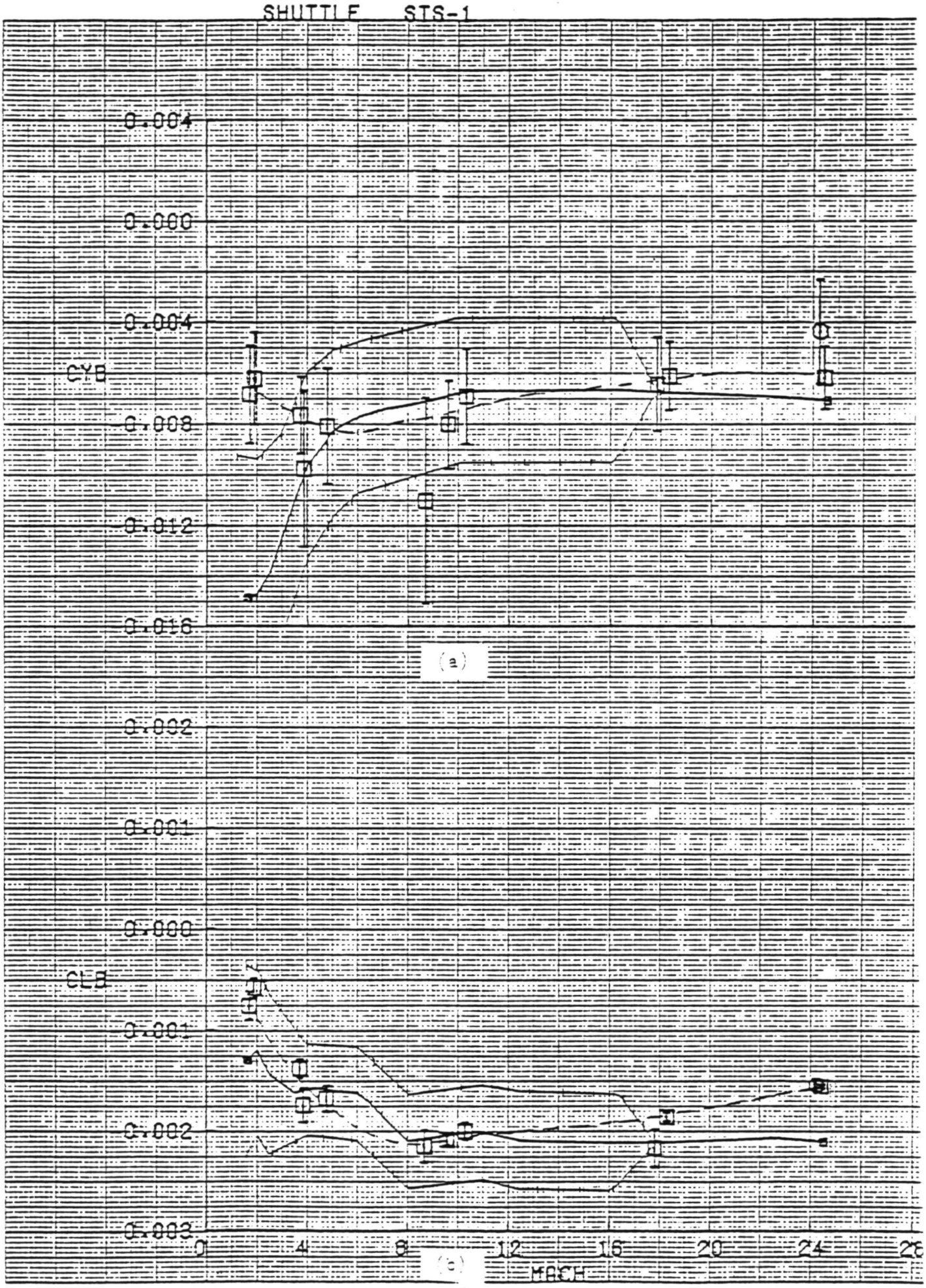

Figure 30. Lateral-directional stability and control derivatives.

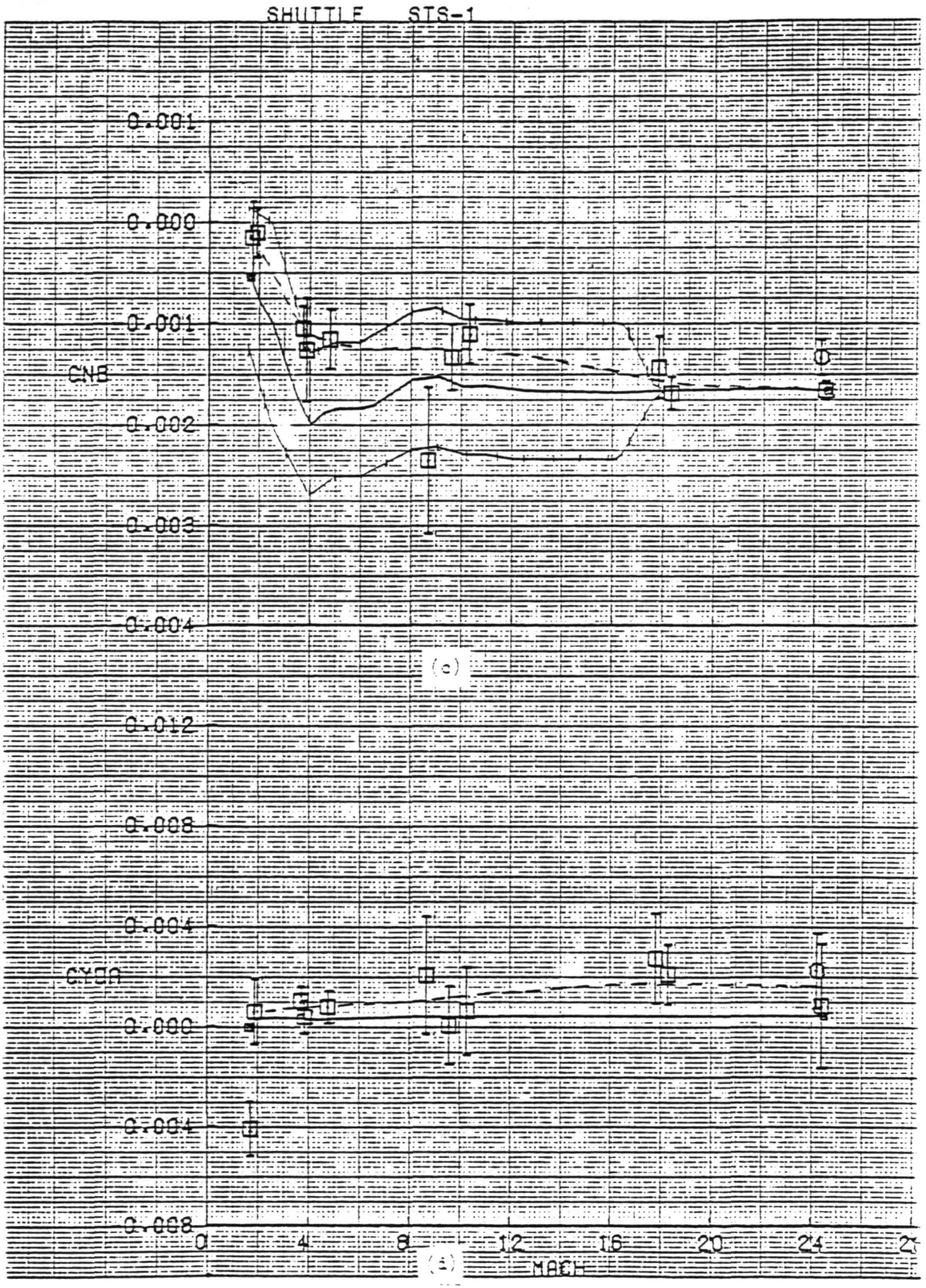

Figure 30 Continued

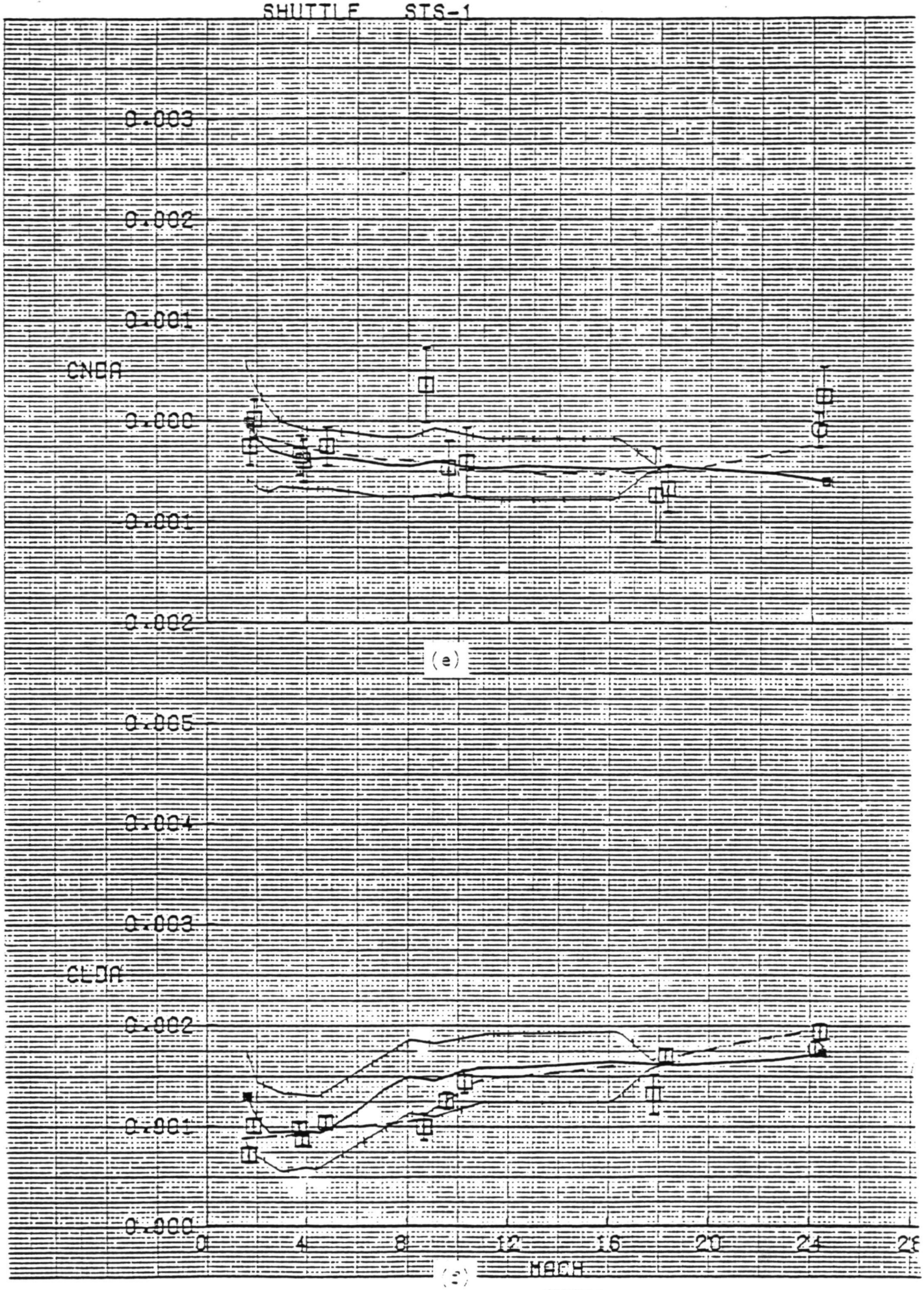

Figure 30. Concluded.

ORIGINAL PAGE IS
OF POOR QUALITY

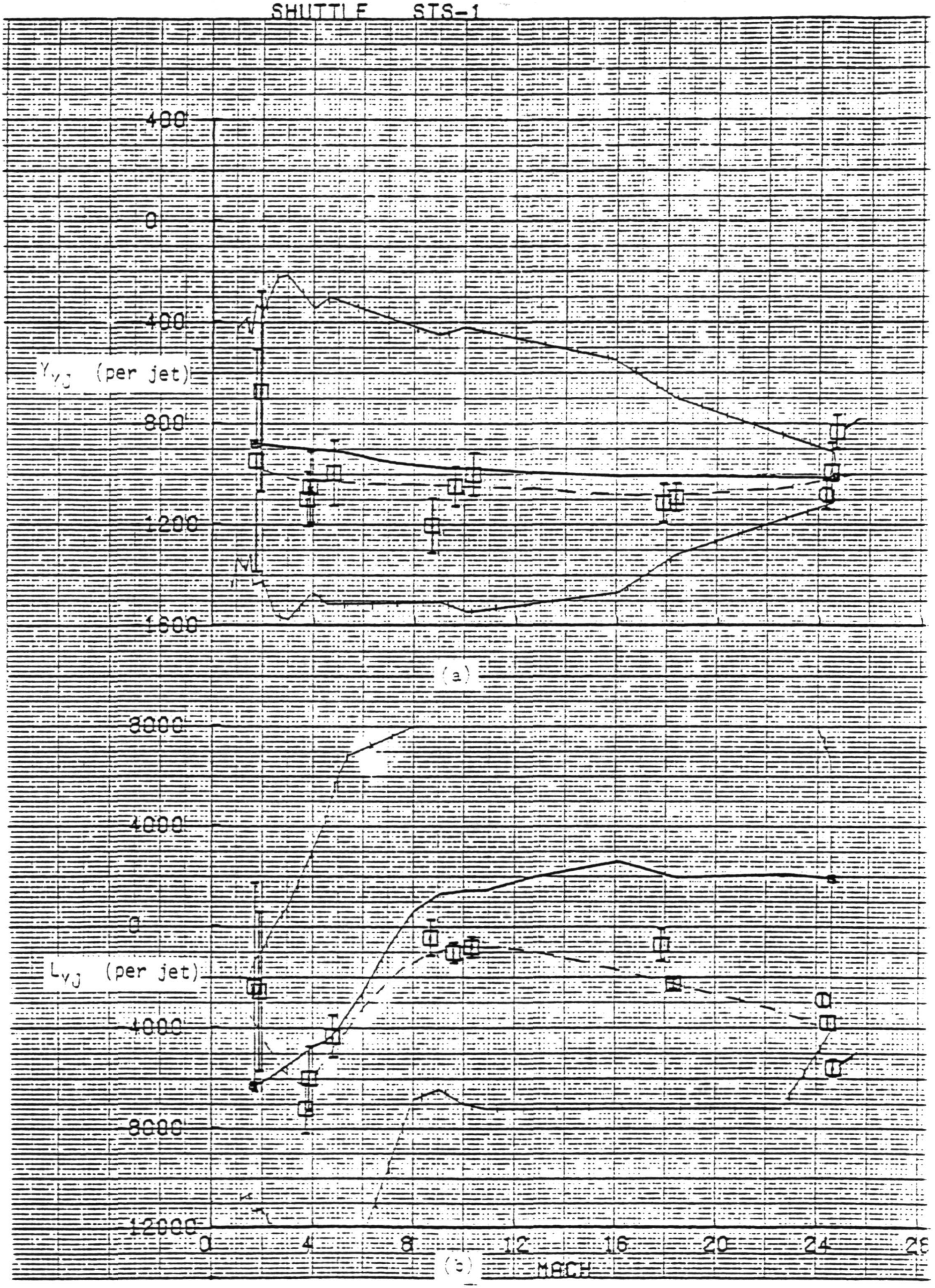

Figure 31. Lateral-directional yaw jet forces and moments.

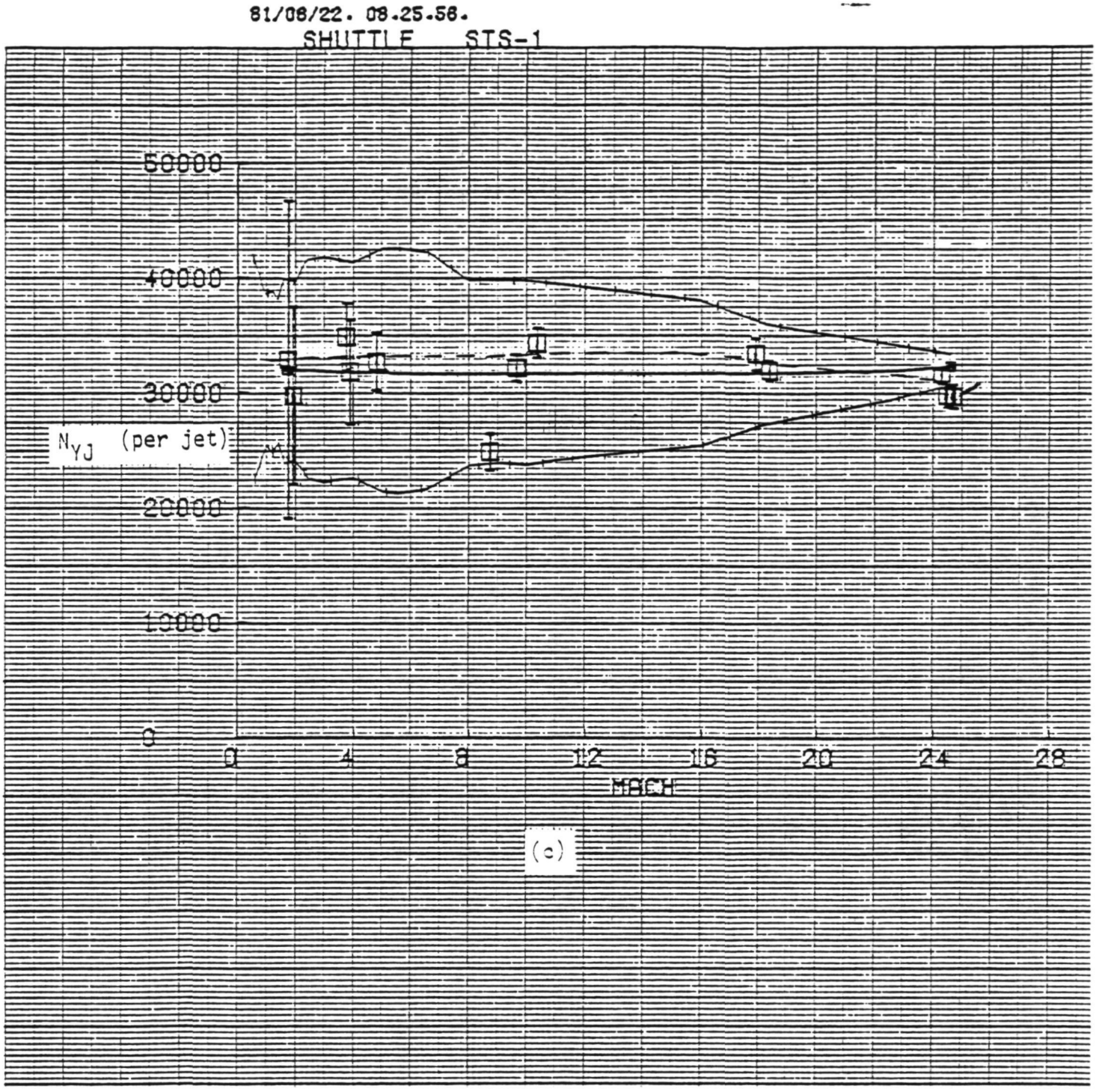

Figure 31. Concluded.

SECTION IV - FLIGHT ANOMALIES

Pre-Interface Rudder Oscillation

From 17:45:40 to 17:47:00 the rudder exhibited a sustained 0.5 Hz oscillation between 0 and 0.1 degree (fig. 32). The reasons for this behavior are not apparent.

M = 24 Pitch Oscillation

A pitch oscillation occurred shortly before the first turn when the aerodynamic surfaces were engaged for pitch control (fig. 33). Because of the body flap mistrim, the body flap was moving from its initial value of 7 degrees to the trim value of 16 degrees. The coupling between the body flap, the pitch jets, and the elevator produced an oscillatory motion which stopped when the body flap reached its trim position. It is recommended that the initial value of body flap be set at 17 degrees for the next flight to reduce the pitch oscillation. Future studies should be made to reduce the elevator/body flap/pitch jet coupling at this flight condition. One possible method would be to engage the body flap as a trimming device before the other aerodynamic surfaces are engaged.

M = 24 Roll Maneuver

The M = 24 turn was characterized by low Dutch-roll damping. Sideslip excursions of 4 degrees were observed. A comparison of the roll response from flight and simulator runs is shown in figure 34. The simulator runs include the nominal aero case, the roll due to yaw jet case, and the case with all of the derivatives modified to match flight values. It can be seen that the primary derivative responsible for the low Dutch-roll damping is the roll due to yaw jet.

For STS-2, the problem could be alleviated to some degree by putting in smaller inputs, thus reducing the excitation of the Dutch-roll mode. In the long term, a control law change will be required to optimize the system for the flight derivatives.

M = 15 Aerodynamic Change

The vehicle encountered an instantaneous 12% axial force increase and pitch trim change at 18:06:18.4 (about 185,000 feet and Mach 15). At the same time a steady sideslip of 0.33 degree developed (fig. 35). These events do not appear to have been precipitated by any control surface or thruster inputs. This is in the regime where viscous effects start to become important. These phenomena may indicate a sudden change in the air flow and shock patterns around the vehicle corresponding to the transition to viscous flow. This event does not appear to be of significant import to flight safety, but it would be very interesting to hypersonic aerodynamics if it were verified that there was a predictable and repeatable flow change.

M = 9 Limit Cycle

A small limit cycle of ±0.2 degree was seen in the elevator at V = 9500 ft/sec (fig. 36). The frequency was about 1 cycle/sec. The oscillation seems to be correlated with the speed brake movement and should be examined in more detail.

M = 2.5 Turn

This maneuver (fig. 37) had more of an oscillatory response in roll rate than the nominal aero data would have predicted. Sideslip excursions were quite small (±0.5 degree). The first part of the maneuver was similar to a roll PTI maneuver, that is, a roll rate command of 5 deg/sec for 6 seconds followed by an abrupt return to near zero roll rate command when the CSS mode was selected. Damping was quite good even with the roll rate oscillation. It is recommended that a roll yaw PTI maneuver be done either slightly before or after this turn on the next flight to properly identify the aerodynamic characteristics.

M = 1 to 2 Roll Oscillation

In this region (fig. 38), a sustained oscillation of ±1 deg/sec in roll rate was observed, which was followed by a divergent tendency which reached an amplitude of ±2 deg/sec. This oscillation was almost entirely in roll, with sideslip excursions of less than ±0.5 degree from the trim value. There was also almost no yaw jet activity: there was one firing in the middle of this period and one at the end, which seemed to damp out the diverging portion of the oscillation.

It would appear that the problem is similar to the M = 2.5 turn and that the sustained oscillation would probably exist only while operating under the threshold of the yaw jets. Since there is insufficient flight aero data in this region to verify this premise at this time, it would be wise to investigate this region in a prudent fashion in the upcoming flights. A recommended procedure to investigate this region is as follows: Perform PTI maneuvers in roll and yaw at M = 3. It would probably be advantageous to let the pilot perform these maneuvers manually and let him do small pulses first and then larger pulses. Repeat these at M = 2 immediately after the turn. If the small pulses give an indication of a sustained oscillation, terminate the tests. Further testing nearer the M = 1 to 1.5 region can be performed if deemed appropriate.

M = 1.5 to 2 Longitudinal Trim

The elevator did not follow the desired schedule in this region (fig. 28) because the body flap could not keep up with the changing trim requirements. This could be alleviated by changing the body flap rate or the deadband logic. However, because of the sensitivity of the lateral-directional characteristics to elevator position, it is recommended that no change be made until the lateral-directional problems in this area are properly identified.

M = 1 Pitch Transient

A small pitch transient occurred at 18:16:34 (fig. 39). This transient was not a result of elevon, body flap, or speed brake inputs. Significant changes in accelerations and static pressures (RCS chamber pressures) occurred at the same time. The transient is probably the result of transonic shock movement. AFFTC radar data indicated that M = 1 at 9 seconds before the transient.

Final Approach and Landing

The landing time history, shown in figure 40, was a very smooth straight in approach to the lakebed runway. Wind and turbulence were minimal. As a result, pilot inputs after preflare were small (less than ±7 degrees in pitch RHC). Elevator rates were generally low. For most of the approach the elevator rates were in the 5 to 10 deg/sec range with occasional peaks to 15 deg/sec. At main gear touchdown, 20 deg/sec was reached momentarily. PIO suppressor activity (PKQ) was calculated using the recorded pitch controller deflection and is shown in figure 40(b). The controller deflections were only sampled at 1 sample per second, and a linear interpolation was made between these points. As a result, the values of PKQ shown are only rough estimates, but they do indicate that the PIO suppressor was hardly activated during this flight.

During the constant equivalent airspeed approach phase, a low frequency oscillation can be seen in airspeed (fig. 40(a)) with an amplitude of ±5 to ±10 knots. This oscillation in combination with the retraction of the speed brakes just prior to preflare resulted in a speed of about 305 knots in the preflare. From figure 26, it can be seen that the L/D increase due to speed brake retraction is greater than predicted, thus adding to this problem. This excess energy produced a landing beyond the desired touchdown point. The tendency to land long was also noted during the ALT flights. It would appear that a more precise aim point, utilizing flight data, should be developed if more accurate touchdowns are to be accomplished with manual control to the runway. The key to low touchdown dispersion is the attainment of the proper stabilized energy state at preflare initiation. This may require that the constant speed portion of the approach be extended to insure stable conditions at the flare initiation, and that the energy state be displayed to the pilot (probably best done on the HUD), so that the proper energy can be achieved and maintained using the speed brakes.

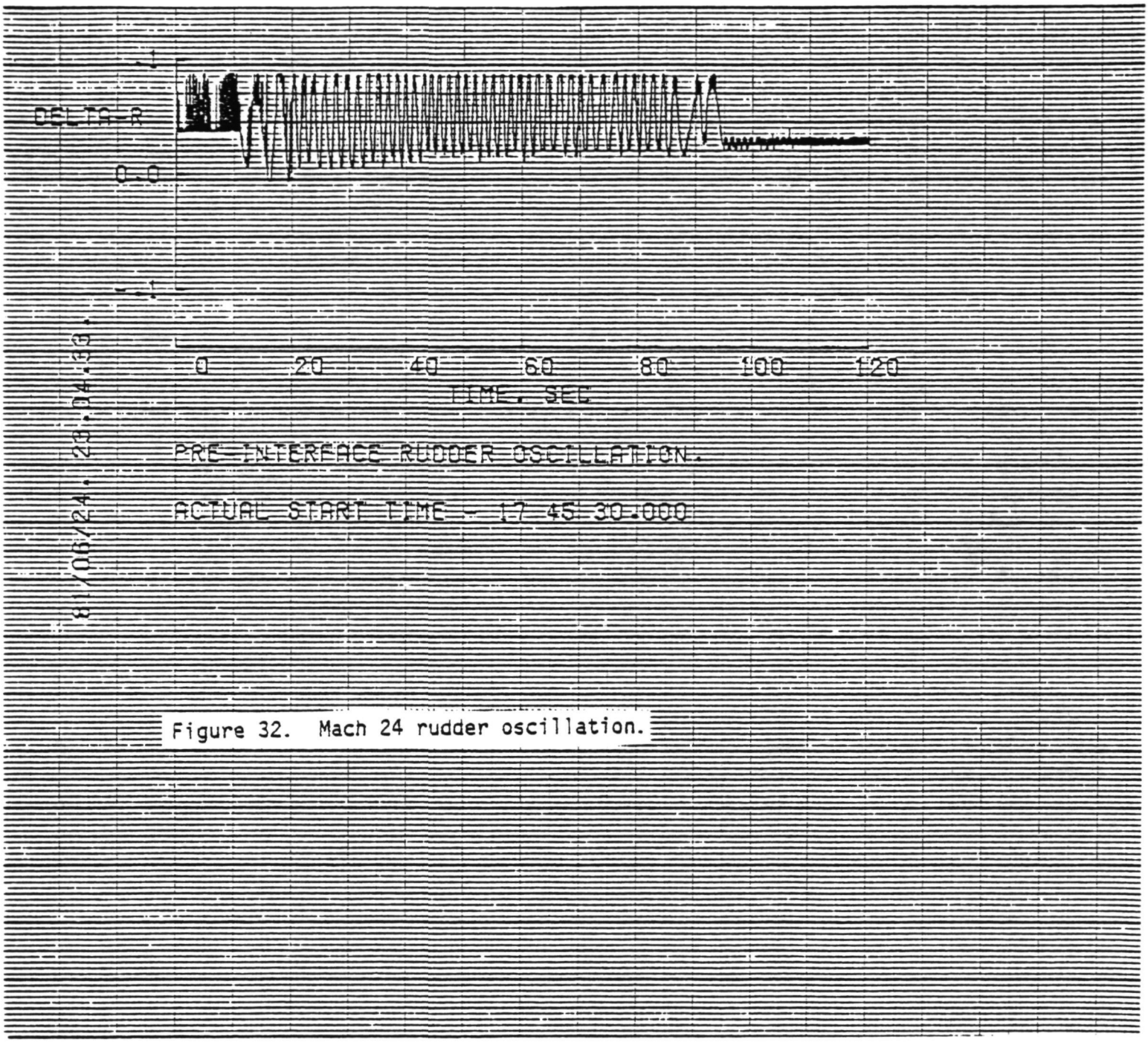

Figure 32. Mach 24 rudder oscillation.

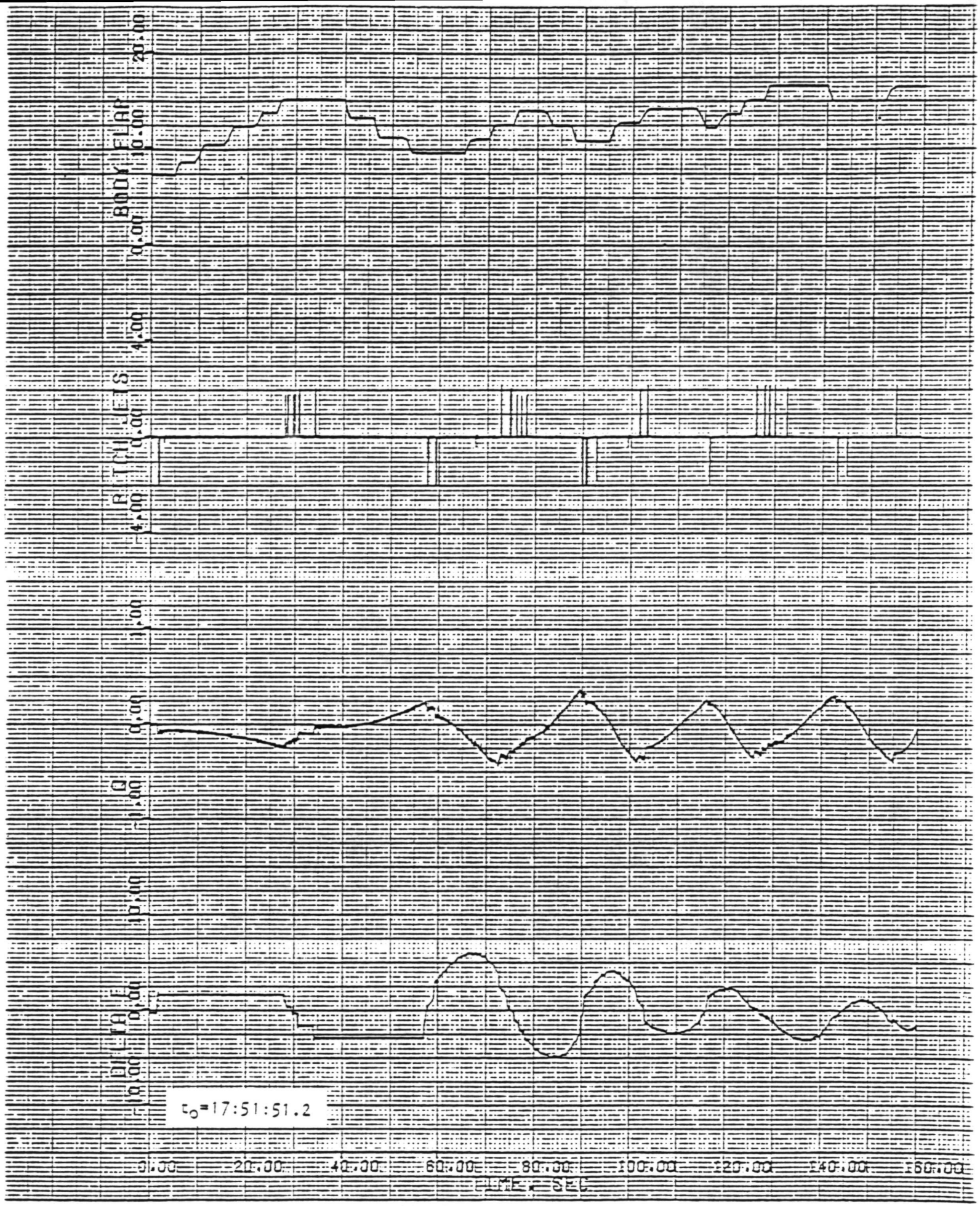

Figure 33. Mach 24 pitch oscillation.

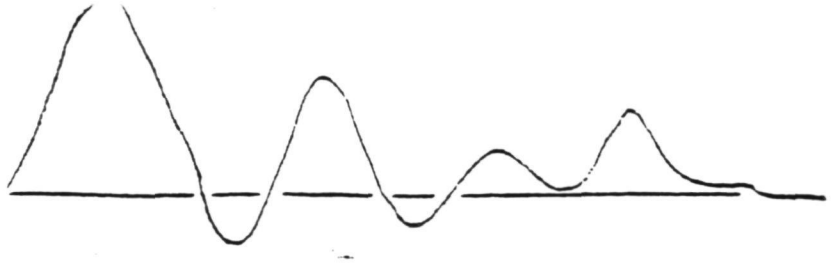

Flight

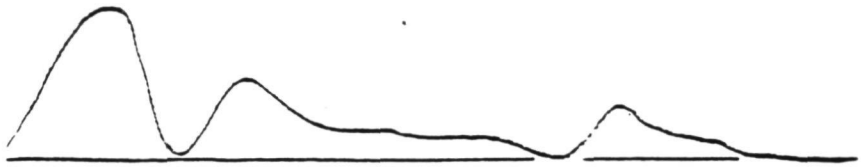

Simulation - nominal aero

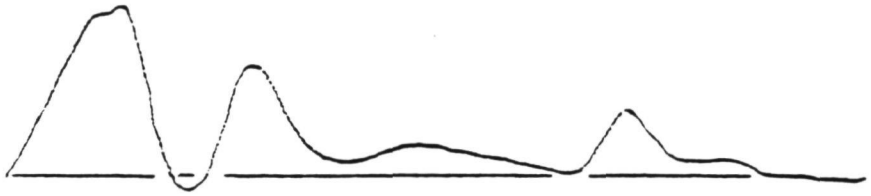

Simulation - Roll due to yawjet

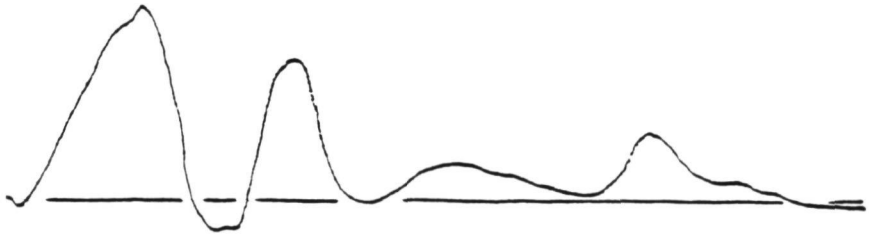

Simulation - Roll due to yawjet & C_{n_β}, C_{y_β}

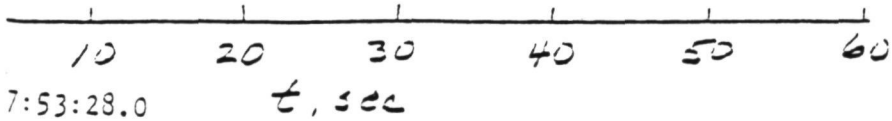

7:53:28.0

w roll damping.
of flight response and simulator response using
l angle commands.

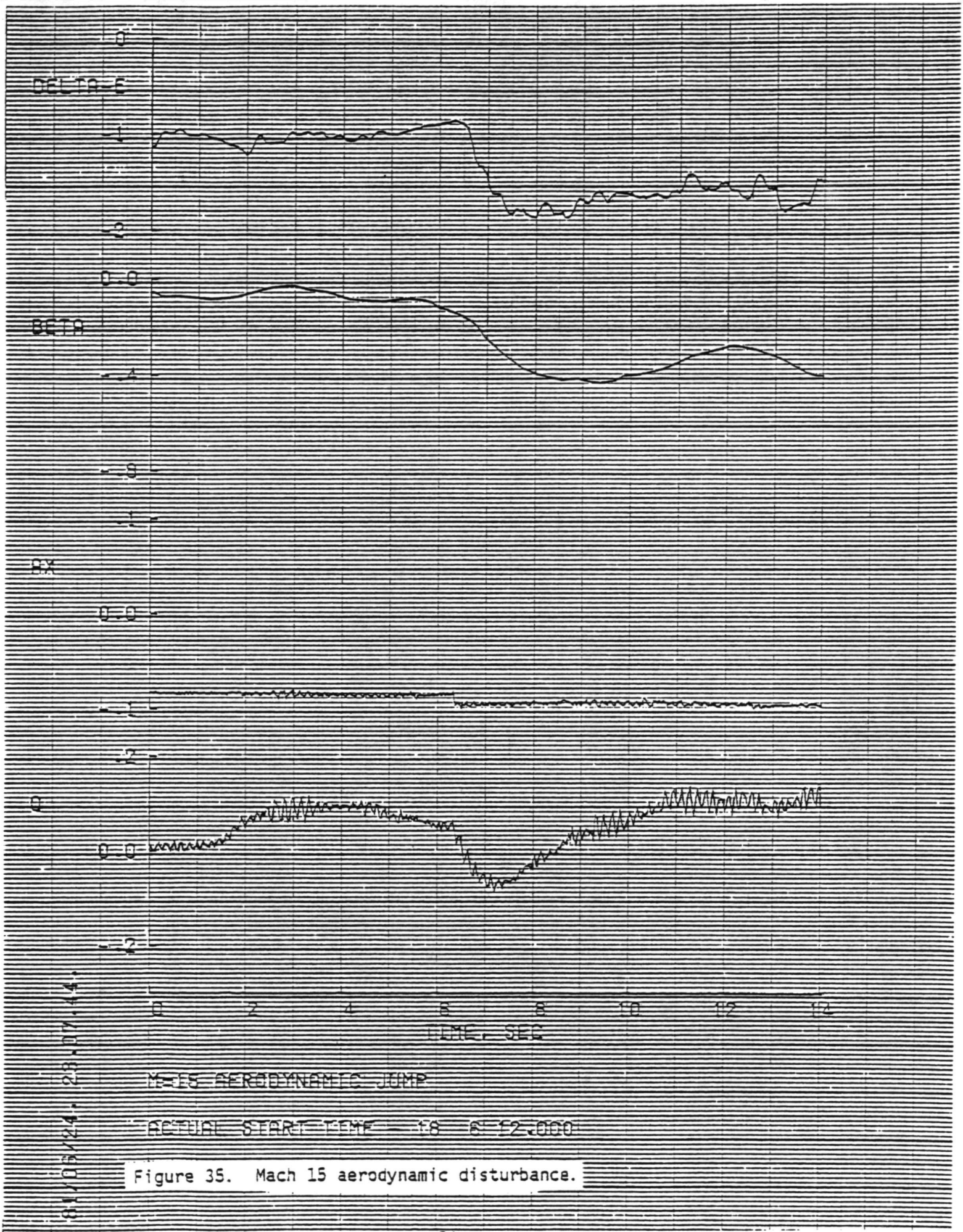

Figure 35. Mach 15 aerodynamic disturbance.

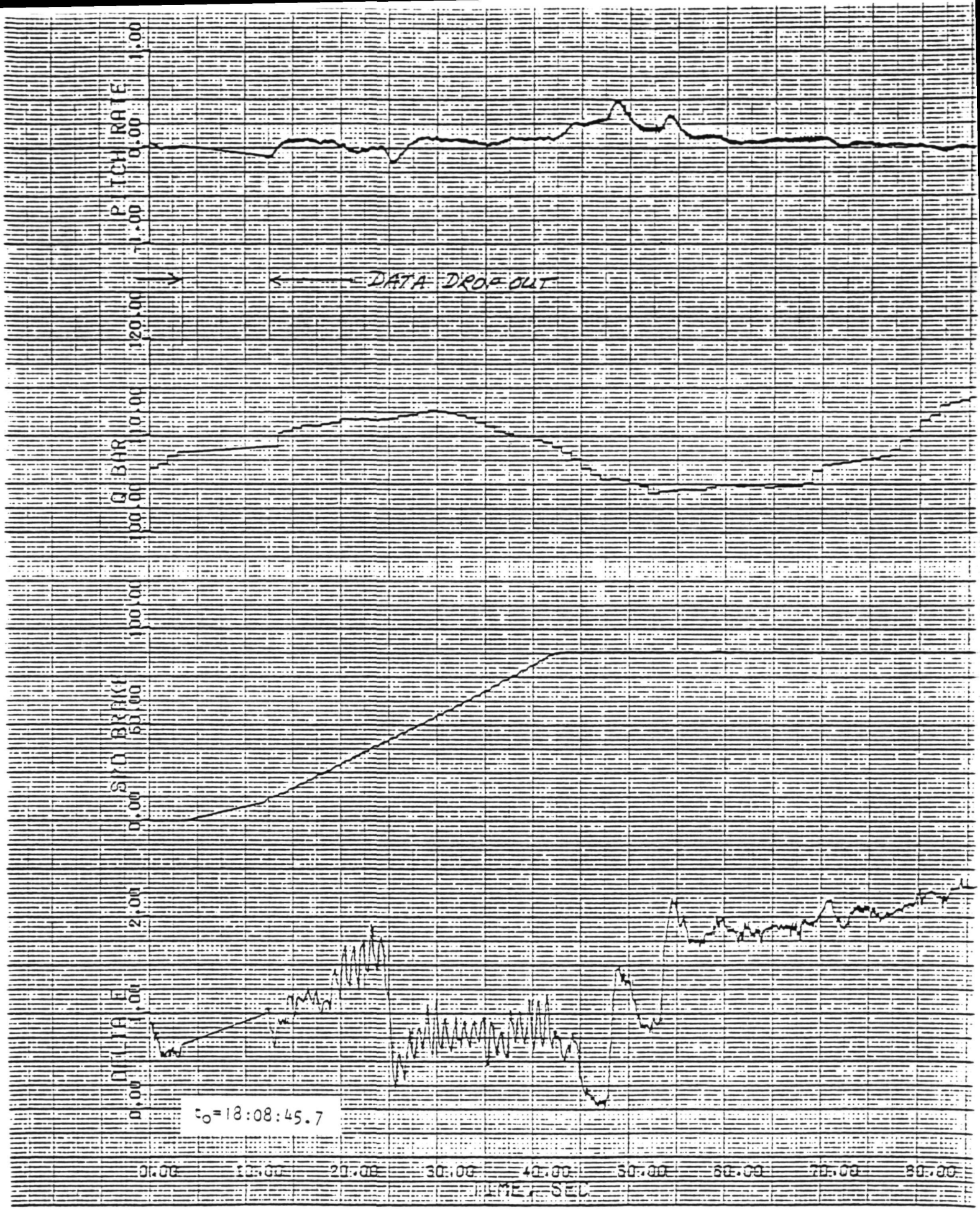

Figure 36. Mach 9 elevator oscillation.

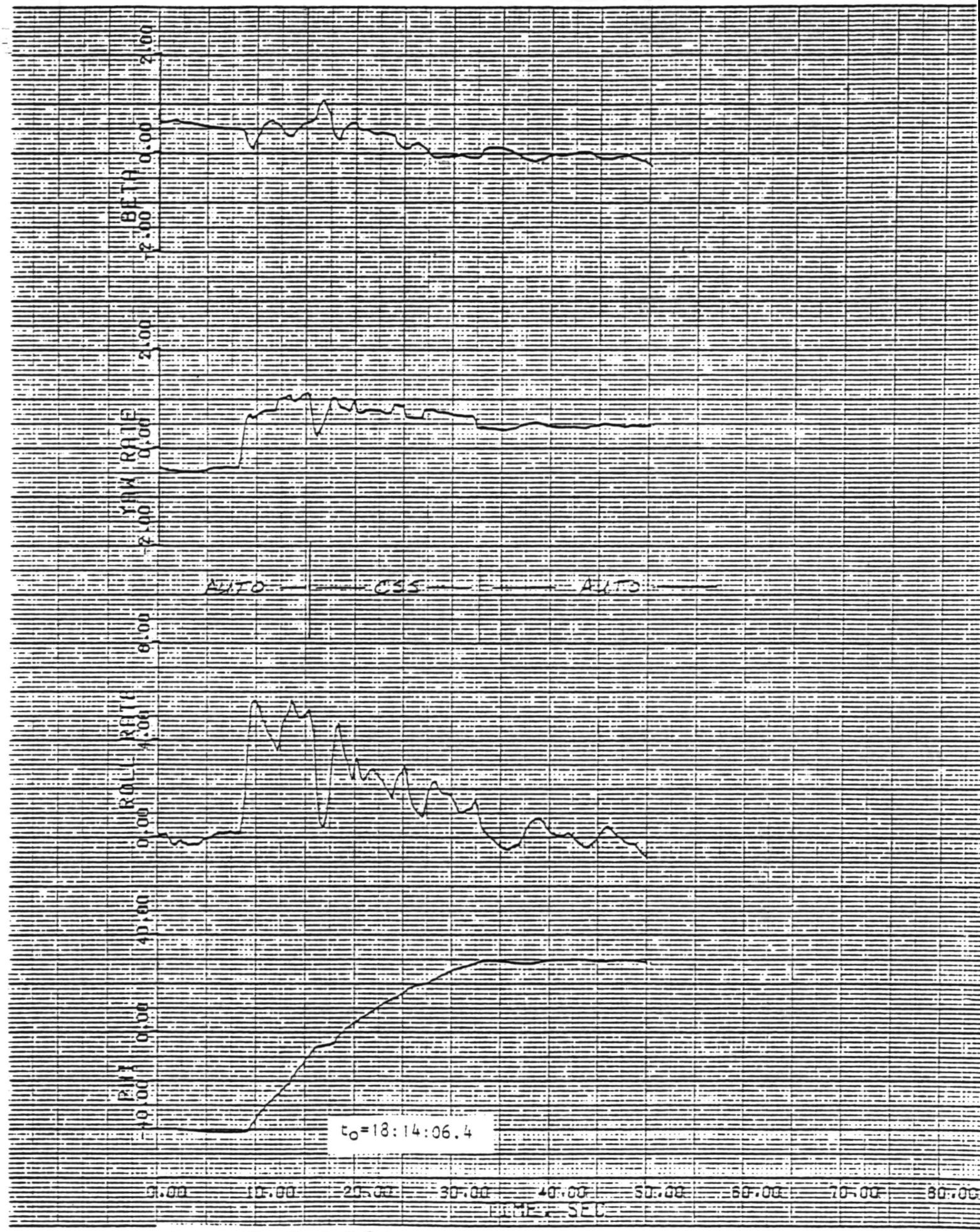

Figure 37. Mach 2.5 turn.

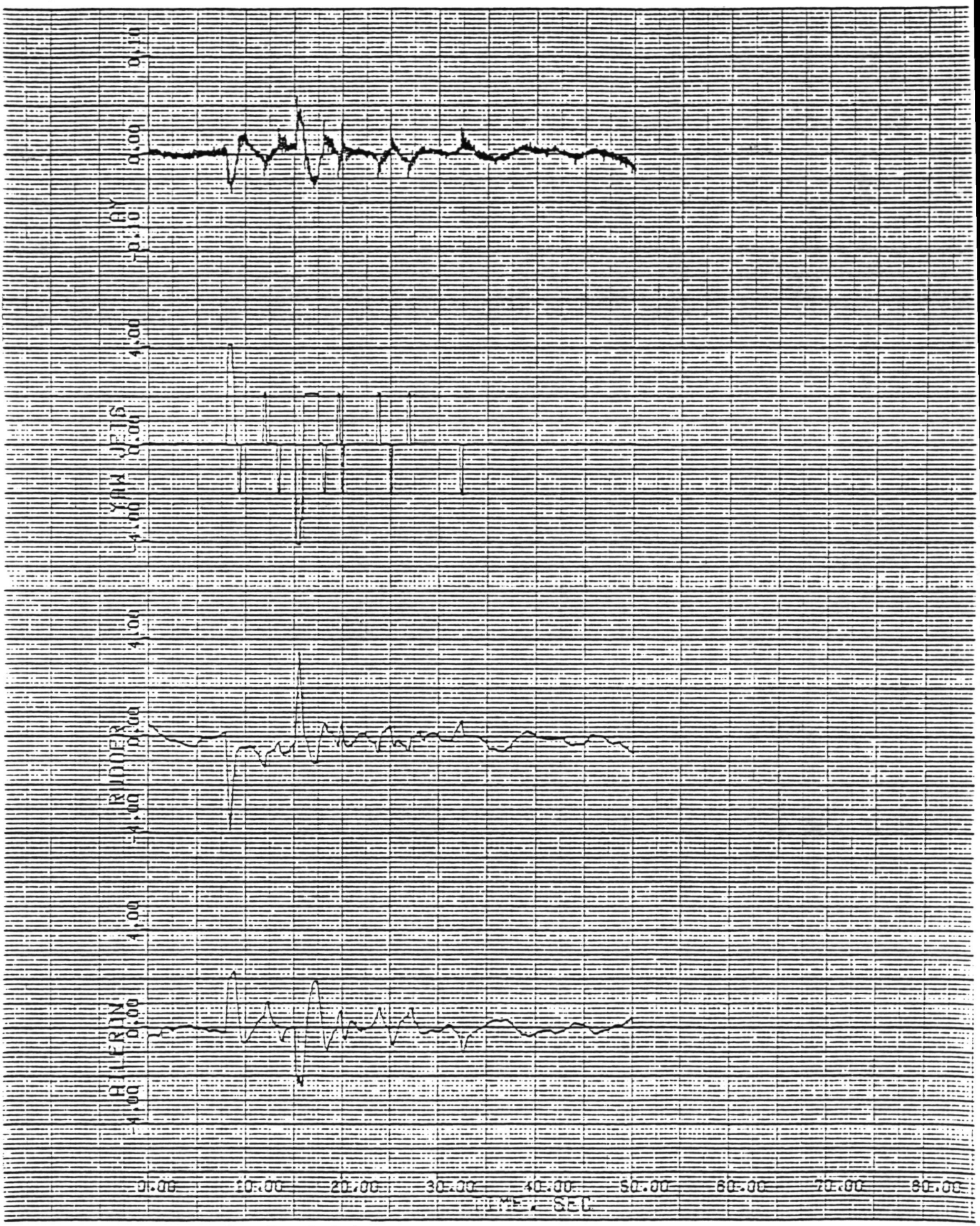

Figure 37. Concluded.

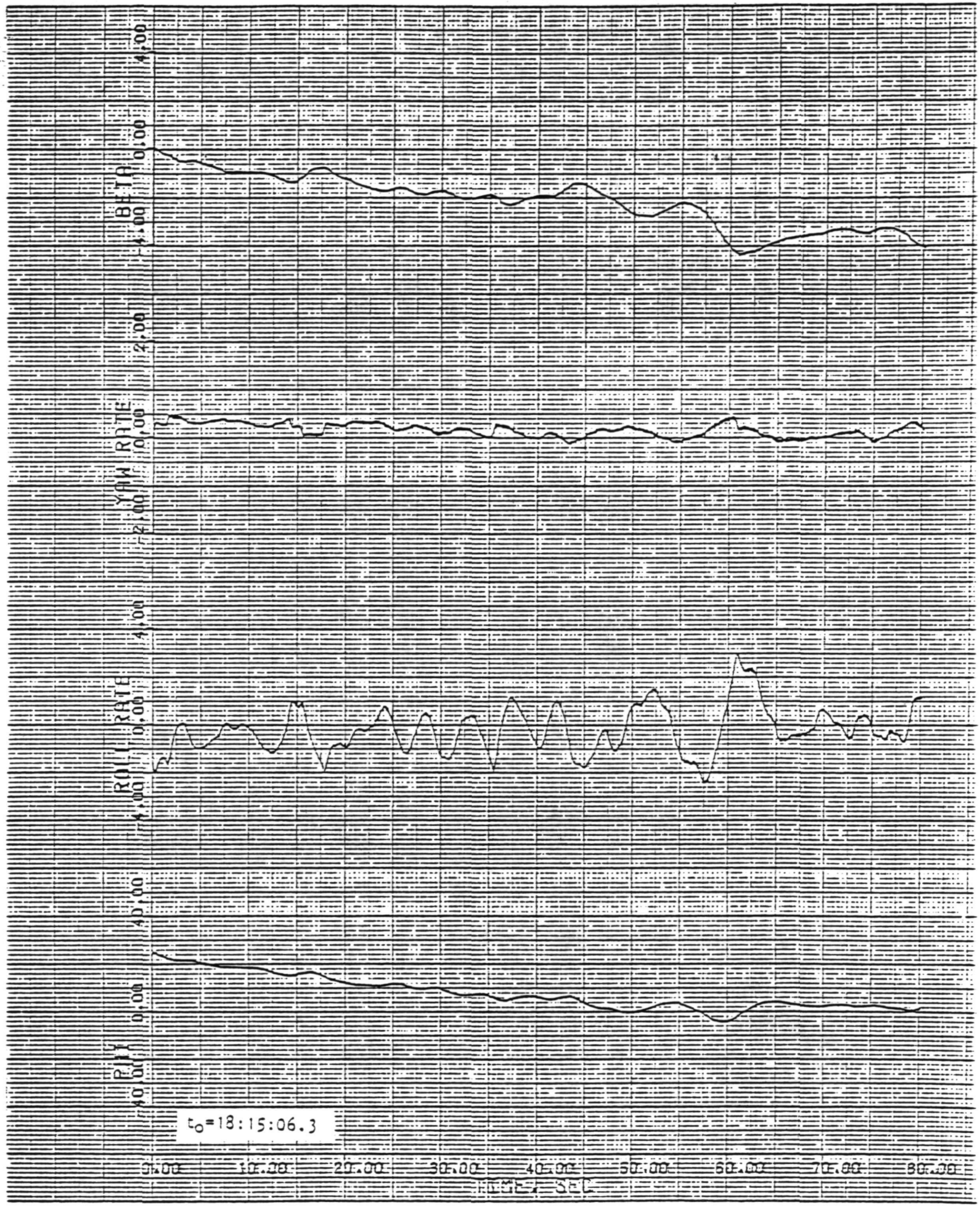

Figure 38. Mach 1 to 2 roll oscillation.

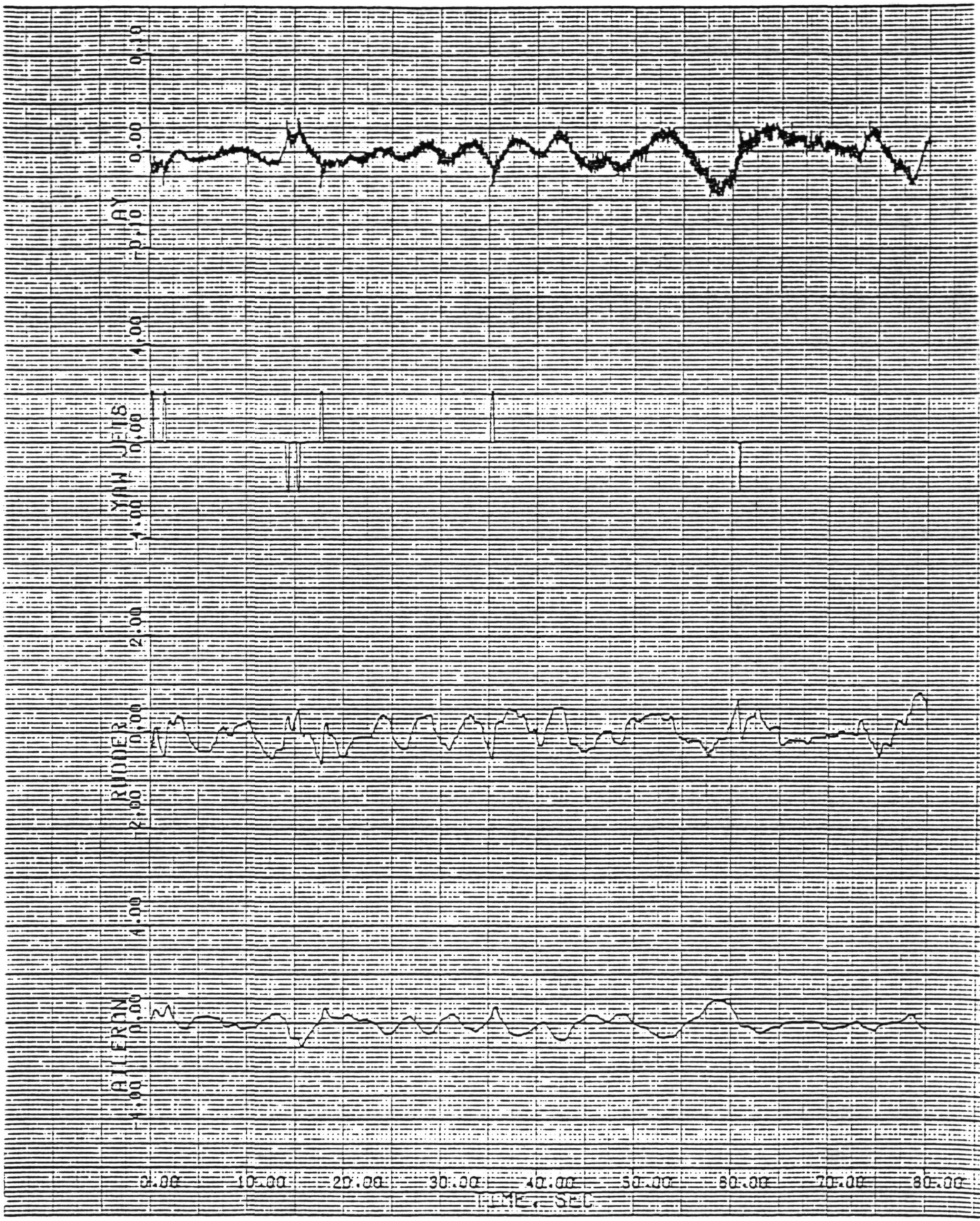

Figure 38. Concluded.

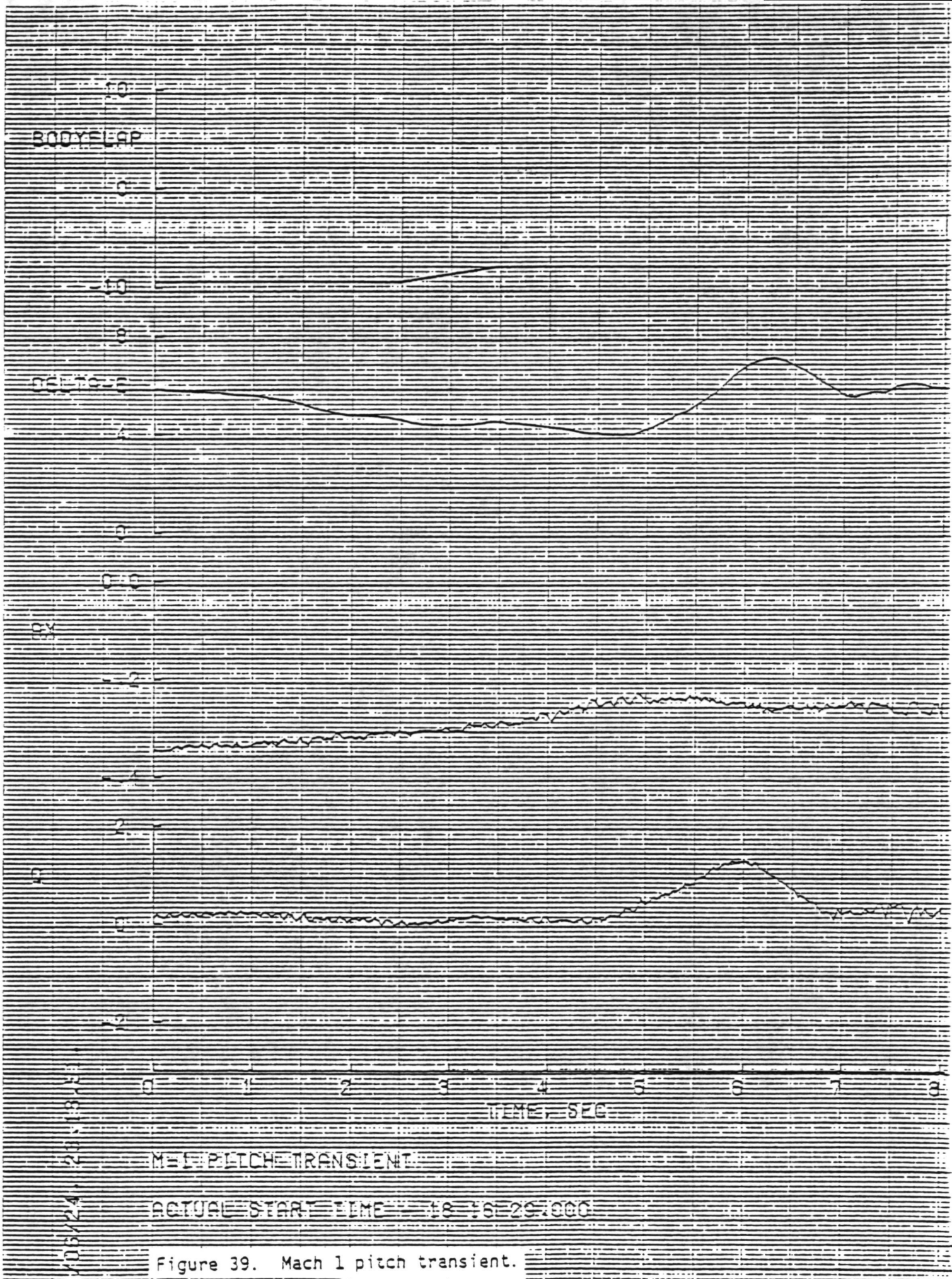

Figure 39. Mach 1 pitch transient.

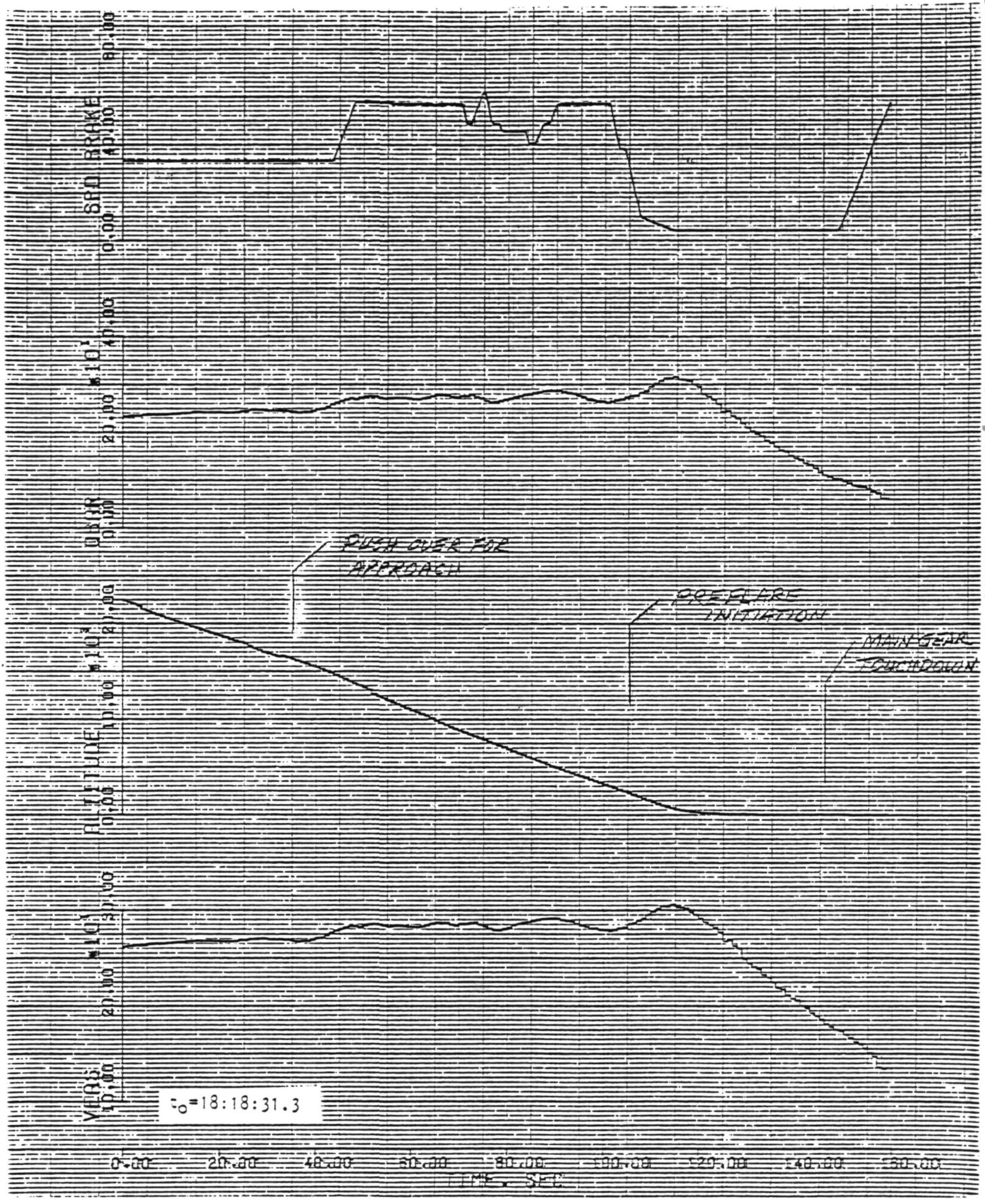

(a)

Figure 40. Approach and landing.

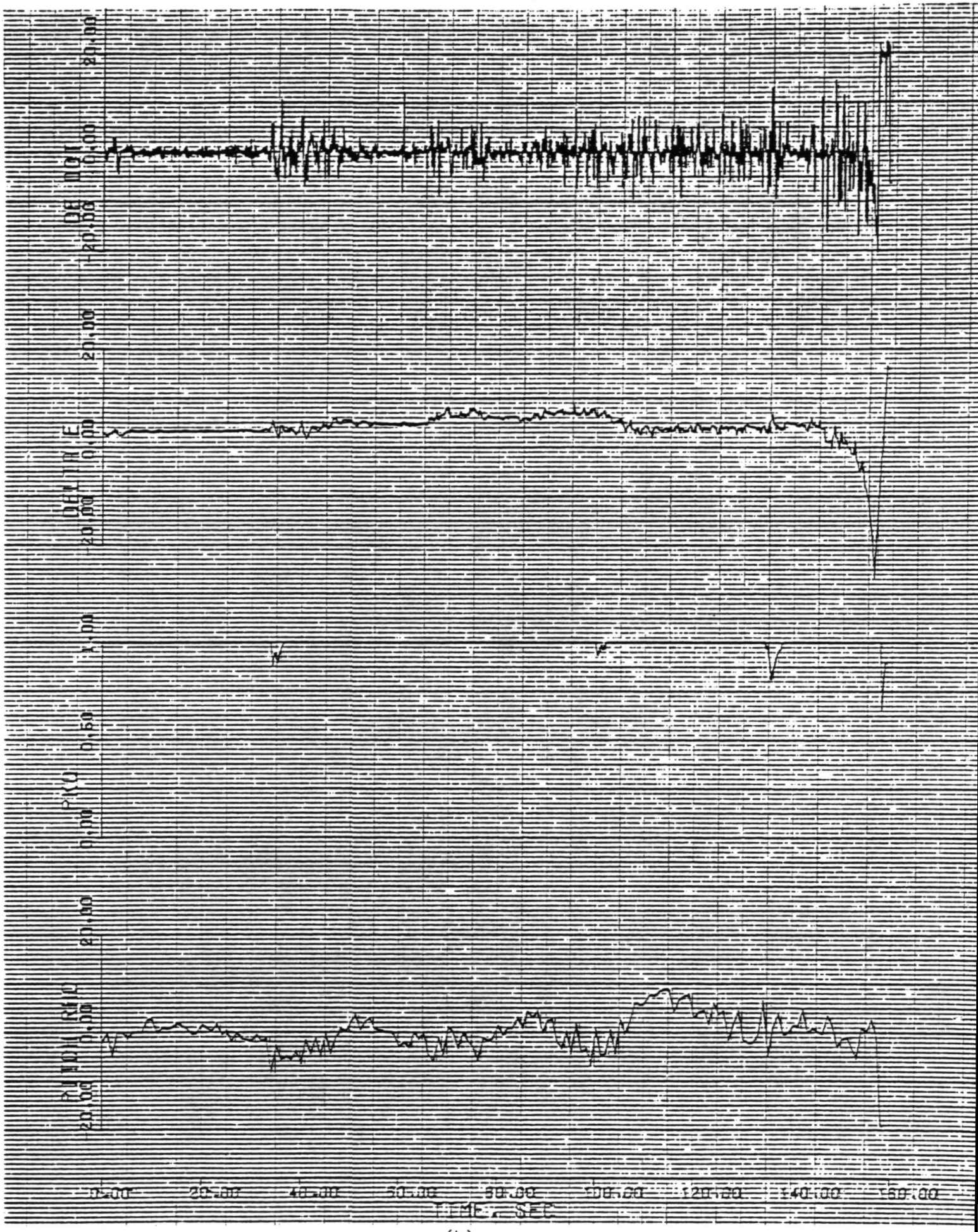

(b)

Figure 40. Continued.

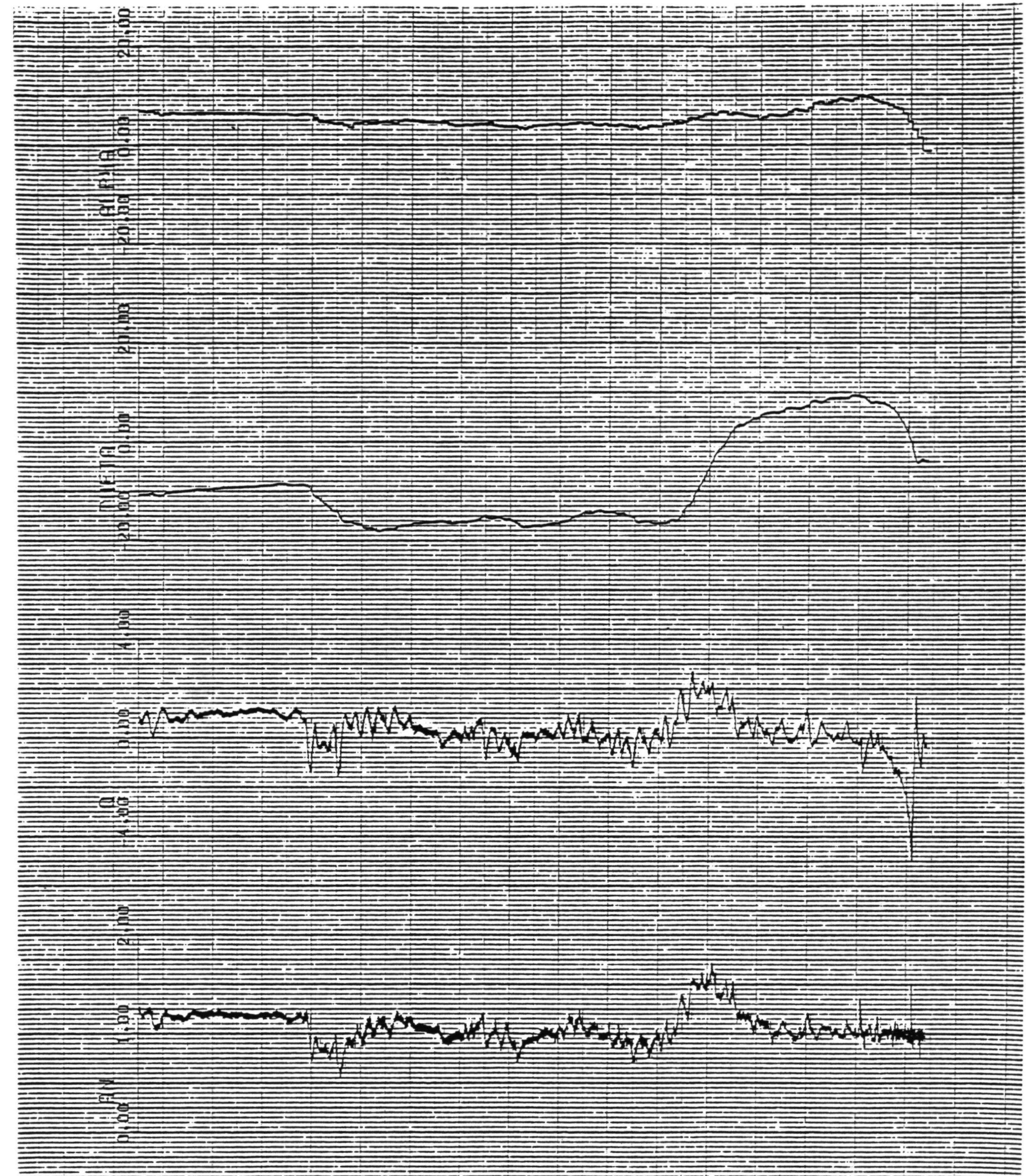

(c)

Figure 40. Concluded.

SECTION V - CONCLUDING REMARKS AND RECOMMENDATIONS

A preliminary analysis of the data acquired during the first shuttle orbiter re-entry (STS-1) had the following results.

Heating levels were lower than predicted. This discrepancy will have to be resolved when additional data become available, perhaps after STS-2, when temperatures will be recorded throughout re-entry.

As indicated in the discussion in section III on stability and control characteristics, several problems compromise the analysis of stability and control data from STS-1. The confidence felt in the stability and control derivatives obtained from STS-1, which were extracted from maneuvers not designed for that purpose, is only fair. Confidence in the derivatives extracted for Mach numbers below 3.5 is especially weak, because these derivatives were affected by sideslip data contaminated by wind and turbulence, nonindependent rudder motions, and buffet. Dryden considers it essential that specific stability and control type maneuvers be performed on subsequent flights to insure that high quality data can be obtained so that realistic entry controllability boundaries can be defined.

Although our results show several discrepancies between predicted and flight values, we would not recommend any changes to the Aerodynamic Data Book values of the stability derivatives for STS-2 flight planning purposes. The rationale is that the quality of the results is only fair to good, and that simulation studies reveal few or no effects of these discrepancies. The one exception is roll due to yaw jet (L_{Y_J}). Our analysis indicates that there is not only a significant difference between predicted and flight values, but also a change in sign above a Mach number of 10. Simulation indicates that this is also the primary derivative responsible for the low Dutch-roll damping evident in the Mach 24 roll maneuver. We would therefore recommend that this discrepancy be taken into account during preparation for STS-2.

We believe it is appropriate to update the aero data for the approach and landing regime with the lift and drag data acquired during the fourth and fifth flights of the approach and landing tests (ALT) as well as from STS-1. It is also recommended that a more precise aim point for energy management prior to preflare be developed based on the flight measurements of lift and drag, and that this be evaluated using the lakebed runway, where long or short landings can be made with less concern.

Finally, we recommend that more highly stressed landings (with crosswinds or turbulence) be performed on the lakebed surface before moving to a paved runway.

SECTION VI - DATA SOURCE AND REFERENCES

The predicted data were obtained on the Dryden simulator using Aero Data Book data. Control deflections used were those measured in flight. Velocity and altitude recorded during the flight were used with a standard atmosphere to determine Mach number and dynamic pressure. No corrections were made to angle of attack or velocity for winds.

The flight data were obtained from real time of the DFI and a copy of the ACIP, OI, and GPC onboard tapes. The data were time shifted using the published time skews. Actuator positions were corrected to surface positions. All flight data analysis used flight recorded values of Mach number and dynamic pressure.

The comparisons made in this report are based on onboard-derived dynamic pressure. Since the stability and control derivative data are only as accurate as the dynamic pressure, the values shown should be considered preliminary.

Dryden Flight Research Center
National Aeronautics and Space Administration
Edwards, California 93523
July 21, 1981

REFERENCES

1. Iliff, Kenneth W.; and Taylor, Lawrence W., Jr.: Determination of Stability Derivatives From Flight Data Using a Newton-Raphson Minimization Technique. NASA TN D-6579, 1972.

2. Maine, Richard E.; and Iliff, Kenneth W.: User's Manual for MMLE3, a General FORTRAN Program for Maximum Likelihood Parameter Estimation. NASA TP-1563, 1980.

3. Maine, Richard E.; and Iliff, Kenneth W.: Formulation and Implementation of a Practical Algorithm for Parameter Estimation With Process and Measurement Noise. AIAA Paper 80-1603, Aug. 1980.

4. Iliff, Kenneth W.; Maine, Richard E.; and Montgomery, T. D.: Important Factors in the Maximum Likelihood Analysis of Flight Test Maneuvers. NASA TP-1459, 1979.

5. Iliff, Kenneth W.: Aircraft Identification Experience. Parameter Identification, AGARD LS-104, Nov. 1979.

1. Report No.	2. Government Accession No.	3. Recipient's Catalog No.
NASA TM-81363		

4. Title and Subtitle	5. Report Date
PRELIMINARY ANALYSIS OF STS-1 ENTRY FLIGHT DATA	August 1981
	6. Performing Organization Code RTOP 989-10-00
7. Author(s)	8. Performing Organization Report No.
	10. Work Unit No.
9. Performing Organization Name and Address Dryden Flight Research Center P.O. Box 273 Edwards, California 93523	11. Contract or Grant No.
	13. Type of Report and Period Covered Technical Memorandum
12. Sponsoring Agency Name and Address National Aeronautics and Space Administration Washington, D.C. 20546	14. Sponsoring Agency Code

15. Supplementary Notes

16. Abstract

Dryden has performed a preliminary analysis of data acquired during the first shuttle orbiter re-entry (STS-1). Heating levels were lower than predicted. This discrepancy will have to be resolved when additional data become available, perhaps after STS-2, when temperatures will be recorded throughout re-entry. The confidence felt in the stability and control derivatives, which were extracted from maneuvers not designed for that purpose, is only fair. Confidence in the derivatives extracted for Mach numbers below 3.5 is especially weak, because these derivatives were affected by sideslip data contaminated by wind and turbulence, nonindependent rudder motions, and buffet. We strongly endorse the existing plans to perform stability and control maneuvers with independent control motions before updating the Aerodynamic Design Data Book or simulators.

We believe it is appropriate to update the aero data for the approach and landing regime with the lift and drag data acquired during the fourth and fifth flights of the approach and landing tests (ALT) as well as from STS-1. Finally, we recommend that more highly stressed landings (with crosswinds or turbulence) be performed on the lakebed surface before moving to a paved runway.

17. Key Words (Suggested by Author(s))	18. Distribution Statement
Orbiter Stability and control Performance Heating Derivative extraction	Unclassified - Unlimited Subject category 18

19. Security Classif. (of this report)	20. Security Classif. (of this page)	21. No. of Pages	22. Price*
Unclassified	Unclassified	73	A05

*For sale by the National Technical Information Service, Springfield, Virginia 22161